HERMETIC PACKAGES AND FEEDTHROUGHS FOR NEURAL PROSTHESES

Quarterly Progress Report # 1

(Contract NIH-NINDS-N01-NS-4-2319)

(Contractor: The Regents of the University of Michigan)

For the Period:

April- June 1998

Submitted to the

Neural Prosthesis Program
National Institute of Neurological Disorders and Stroke
National Institutes of Health

By the

Center For Integrated Sensors and Circuits
Department of Electrical Engineering and Computer Science
University of Michigan
Ann Arbor, Michigan 48109-2122

Program Personnel:

UNIVERSITY OF MICHIGAN

Faculty:
Professor Khalil Najafi: Principal Investigator
Professor David J. Anderson, Biological Experiments

Staff:
Mr. James Wiler: Animal Implants and Surgery

Graduate Student Research Assistants:
Mr. Mehmet Dokmeci: Packaging and Accelerated Testing
Mr. Sebastien Hauverspre: Package Fabrication and Testing

July 1998

SUMMARY

During the past quarter we continued testing of glass packages under accelerated conditions, conducted a detailed literature survey on accelerated testing, designed and started the fabrication of a polyimide-based humidity sensor. and also developed analytical models for remote monitoring of humidity inside the glass packages using telemetry.

Our most significant package testing results to date are those obtained from a series of silicon-glass packages that have been soaking in DI water at 85°C and 95°C for more than a year. We reported in the last progress reports that all packages soaking at 95°C had failed. There were also 2 packages that were soaking at 85°C. Both of these two packages are still dry and under test. Of the original 10 packages, the longest going sample has reached a maximum of 1347 days at 85°C and 484 days at 95°C. If we assume that all of the packages at 85°C failed the same time that the 95°C packages failed, we can calculate a worst case mean time to failure of 258 days for the samples at 85°C, and of 119 days for the samples soaking at 95°C. The worst case MTTF at body temperature based on these tests is then calculated to be 59 years. These tests have been very encouraging and clearly indicate the packages can last for many years in water. In addition to these tests in DI water, we had also soaked several packages in ***saline*** at the above two temperatures. The results obtained from these tests were reported in the last progress report. We also have had 4 packages soaking at room temperature in saline. The longest lasting package has been soaking for 1247 days, and an average soak period of 1022 days at room temperature. We will continue to observe these packages for any sign of leakage. A new set of package tests had also been initiated in the previous quarter at 85 and 95°C. At each temperature, eight packages that had been coated with silicone to prevent premature dissolution of the top polysilicon bonding layer were soaked. These tests have provided a MTTF of 212 days at 85°C, and 125 days at 95°C, and these results indicate again the problem we have had with the dissolution of the polysilicon film. However, these results also show that the silicone coating significantly reduces the time to failure of these coated packages. We have reported possible means to prevent this dissolution and will begin to test and implement some of these techniques so we can circumvent this failure mode (which is a consequence of the testing technique used).

A polyimide humidity sensor based on a simple capacitive structure has been designed and is now in fabrication. We will use these sensors to monitor the humidity inside the package in actual animal experiments. These sensors are expected to be finished at the end of next quarter.

We have also completed the modeling and study of a simple telemetry technique for remote monitoring of changes in dew point inside the package. This is based on the integrated on-chip coil which is inductively coupled to an external transmitter coil. Calculations and preliminary tests are being conducted to determine whether changes in the impedance of the dew point sensor can be detected reliably using the external transmitter without the need for an integrated internal transmitter. Additional results will be provided in this area in the coming quarter.

1. INTRODUCTION

This project aims at the development of hermetic, biocompatible micropackages and feedthroughs for use in a variety of implantable neural prostheses for sensory and motor handicapped individuals. In addition, it will also develop a telemetry system for monitoring package humidity in unrestrained animals, and of telemetry electronics and packaging for stimulation of peripheral nerves. The primary objectives of the proposed research are: 1) the development and characterization of hermetic packages for miniature, silicon-based, implantable neural prostheses designed to interface with the nervous system for many decades; 2) the development of techniques for providing multiple sealed feedthroughs for the hermetic package; 3) the development of custom-designed packages and systems used in several different chronic stimulation or recording applications in the central or peripheral nervous systems in collaboration and cooperation with groups actively involved in developing such systems; and 4) establishing the functionality and biocompatibility of these custom-designed packages in *in-vivo* applications. Although the proposed research is focused on the development of the package and feedthroughs, it also aims at the development of inductively powered systems that can be used in many implantable recording and stimulation devices in general, and of multichannel microstimulators for functional neuromuscular stimulation, and multichannel recording microprobes for CNS applications in particular.

Our group here at the Center for Integrated Sensors and Circuits at the University of Michigan has been involved in the development of silicon-based multichannel recording and stimulating microprobes for use in the central and peripheral nervous systems. More specifically, during the past three contract periods dealing with the development of a single-channel inductively powered microstimulator, our research and development program has made considerable progress in a number of areas related to the above goals. A hermetic packaging technique based on electrostatic bonding of a custom-made glass capsule and a supporting silicon substrate has been developed and has been shown to be hermetic for a period of at least a few decades in salt water environments. This technique allows the transfer of multiple interconnect leads between electronic circuitry and hybrid components located in the sealed interior of the capsule and electrodes located outside of the capsule. The glass capsule can be fabricated using a variety of materials and can be made to have arbitrary dimensions as small as 1.8mm in diameter. A multiple sealed feedthrough technology has been developed that allows the transfer of electrical signals through polysilicon conductor lines located on a silicon support substrate. Many feedthroughs can be fabricated in a small area. The packaging and feedthrough techniques utilize biocompatible materials and can be integrated with a variety of micromachined silicon structures.

The general requirements of the hermetic packages and feedthroughs to be developed under this project are summarized in Table 1. Under this project we will concentrate our efforts to satisfy these requirements and to achieve the goals outlined above. There are a variety of neural prostheses used in different applications, each having different requirements for the package, the feedthroughs, and the particular system application. The overall goal of the program is to develop a miniature hermetic package that can seal a variety of electronic components such as capacitors and coils, and integrated circuits and sensors (in particular electrodes) used in neural prostheses. Although the applications are different, it is possible to identify a number of common requirements in all of these applications in addition to those requirements listed in Table 1. The packaging and feedthrough technology should be capable of:

1- protecting non-planar electronic components such as capacitors and coils, which typically have large dimensions of about a few millimeters, without damaging them;
2- protecting circuit chips that are either integrated monolithically or attached in a hybrid fashion with the substrate that supports the sensors used in the implant;
3- interfacing with structures that contain either thin-film silicon microelectrodes or conventional microelectrodes that are attached to the structure;

Table 1: General Requirements for Miniature Hermetic Packages and Feedthroughs for Neural Prostheses Applications

Package Lifetime:

≥ 40 Years in Biological Environments @ 37°C

Packaging Temperature:

≤360°C

Package Volume:

10-100 cubic millimeters

Package Material:

Biocompatible
Transparent to Light
Transparent to RF Signals

Package Technology:

Batch Manufacturable

Package Testability:

Capable of Remote Monitoring
In-Situ Sensors (Humidity & Others)

Feedthroughs:

At Least 12 with ≤125μm Pitch
Compatible with Integrated or Hybrid Microelectrodes
Sealed Against Leakage

Testing Protocols:

In-Vitro Under Accelerated Conditions
In-Vivo in Chronic Recording/Stimulation Applications

We have identified two general categories of packages that need to be developed for implantable neural prostheses. The first deals with those systems that contain large components like capacitors, coils, and perhaps hybrid integrated circuit chips. The second deals with those systems that contain only integrated circuit chips that are either integrated in the substrate or are attached in a hybrid fashion to the system.

Figure 1 shows our general proposed approach for the package required in the first category. This figure shows top and cross-sectional views of our proposed approach here. The package is a glass capsule that is electrostatically sealed to a support silicon substrate. Inside the glass capsule are housed all of the necessary components for the system. The electronic circuitry needed for any analog or digital circuit functions is either fabricated on a separate circuit chip that is hybrid mounted on the silicon substrate and electrically connected to the silicon substrate, or integrated monolithically in the support silicon substrate itself. The attachment of the hybrid IC chip to the silicon substrate can be performed using a number of different technologies such as simple wire bonding between pads located on each substrate, or using more sophisticated techniques such as flip-chip solder reflow or tab bonding. The larger capacitor or microcoil components are mounted on either the substrate or the IC chip using appropriate epoxies or solders. This completes the assembly of the electronic components of the system and it should be possible to test the system electronically at this point before the package is completed. After testing, the system is packaged by placing the glass capsule over the entire system and bonding it to the silicon substrate using an electrostatic sealing process. The cavity inside the glass package is now hermetically sealed against the outside environment. Feedthroughs to the outside world are provided using the grid-feedthrough technique discussed in previous reports. These feedthroughs transfer the electrical signals between the electronics inside the package and various elements outside of the package. If the package has to interface with conventional microelectrodes, these microelectrodes can be attached to bonding pads located outside of the package; the bond junctions will have to be protected from the external environment using various polymeric encapsulants. If the package has to interface with on-chip electrodes, it can do so by integrating the electrode on the silicon support substrate. Interconnection is simply achieved using on-chip polysilicon conductors that make the feedthroughs themselves. If the package has to interface with remotely located recording or stimulating electrodes that are attached to the package using a silicon ribbon cable, it can do so by integrating the cable and the electrodes again with the silicon support substrate that houses the package and the electronic components within it.

Figure 2 shows our proposed approach to package development for the second category of applications. In these applications, there are no large components such as capacitors and coils. The only component that needs to be hermetically protected is the electronic circuitry. This circuitry is either monolithically fabricated in the silicon substrate that supports the electrodes (similar to the active multichannel probes being developed by the Michigan group), or is hybrid attached to the silicon substrate that supports the electrodes (like the passive probes being developed by the Michigan group). In both of these cases the package is again another glass capsule that is electrostatically sealed to the silicon substrate. Notice that in this case, the glass package need not be a high profile capsule, but rather it need only have a cavity that is deep enough to allow for the silicon chip to reside within it. Note that although the silicon IC chip is originally 500μm thick, it can be thinned down to about 100μm, or can be recessed in a cavity created in the silicon substrate itself. In either case, the recess in the glass is less than 100μm deep (as opposed to several millimeters for the glass capsule). Such a glass package can be easily fabricated in a batch process from a larger glass wafer.

The above two approaches address the needs for most implantable neural prostheses. Note that both of these techniques utilize a silicon substrate as the supporting base, and are not directly applicable to structures that use other materials such as ceramics or metals. Although this may seem a limitation at first, we believe that the use of silicon is, in fact, an advantage because it is biocompatible and many emerging systems use silicon as a support substrate.

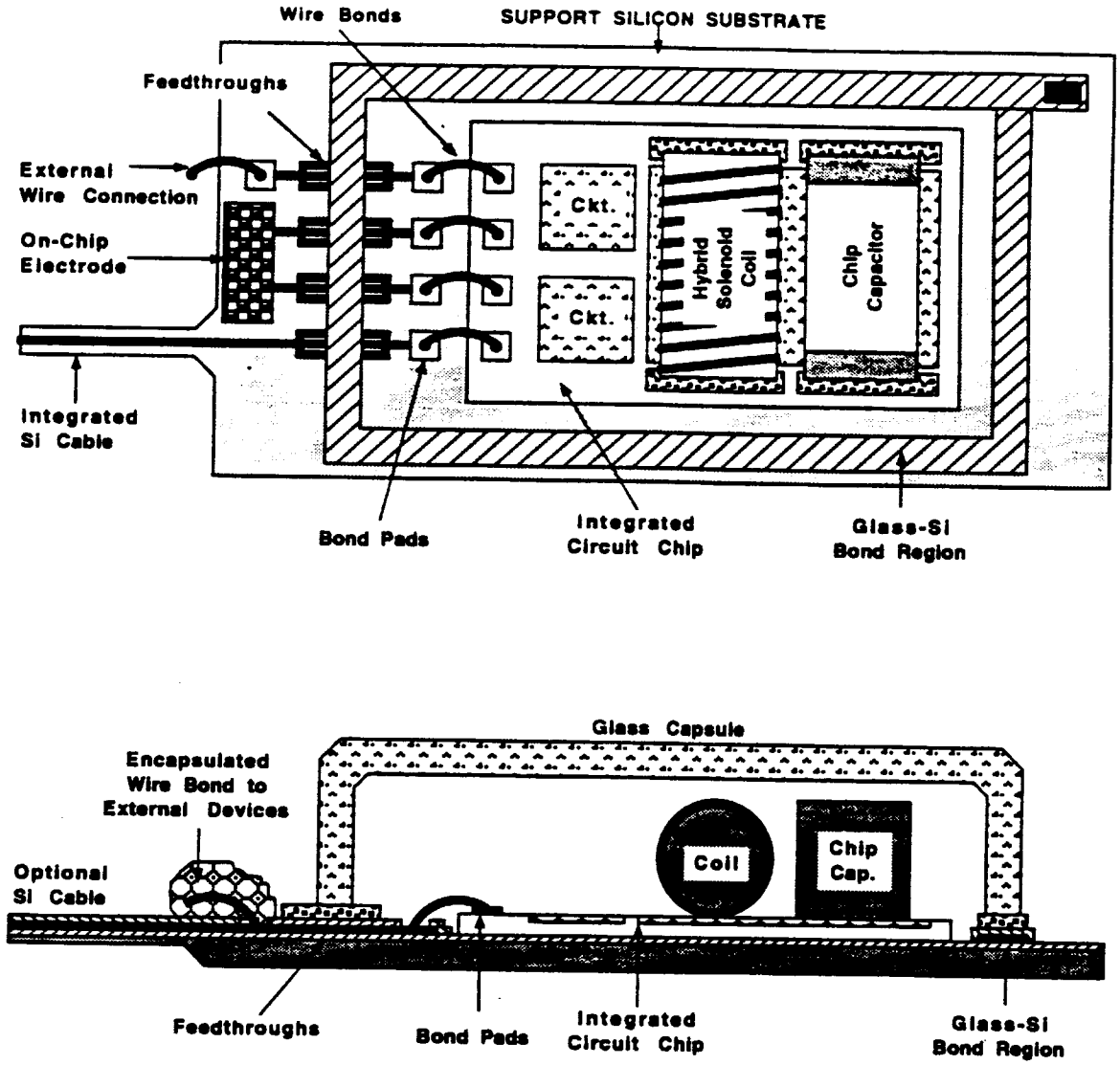

Figure 1: A generic approach for packaging implantable neural prostheses that contain a variety of components such as chip capacitors, microcoils, and integrated circuit chips. This packaging approach allows for connecting to a variety of electrodes.

We will further improve the silicon glass package and its built-in feedthroughs, and will study and explore alternative technologies for hermetic packaging of implantable systems. In particular, we have proposed using a silicon capsule that can be electrostatically bonded to a silicon substrate thus allowing the capsule to be machined down to dimensions below a 100μm. We will also develop an implantable telemetry system for monitoring package humidity in unrestrained animals for a period of at least one year. Two separate systems have been proposed, one based on a simple oscillator, and the other based on a switched-capacitor readout interface circuit and an on-chip low-power AD converter, both using a polyimide-based humidity sensor. This second system will telemeter the humidity information to an outside receiver using a 300MHz on-chip transmitter.

Finally, we have forged potential collaborations with two groups working in the development of recording/stimulating systems for neural prostheses. The first group is that led by Professor Ken Wise at the University of Michigan, which has been involved in the development of miniature, silicon-based multichannel recording and stimulation system for the CNS for many years. Through this collaboration we intend to develop hermetic packages and feedthroughs for a 3-D recording/stimulation system that is under development at Michigan. We will also develop the telemetry front end necessary to deliver power and data to this system. The second group is at Case Western Reserve University, led by Prof. D. Durand, and has been involved in recording and stimulation from peripheral nerves using cuff electrodes. Through this collaboration we intend to develop a fully-integrated, low-profile, multichannel, hermetic, wireless peripheral nerve stimulator that can be used with their nerve cuff electrode. This system can be directly used with other nerve cuffs that a number of other groups around the country have developed. Both of these collaborations should provide us with significant data on the reliability and biocompatibility of the package.

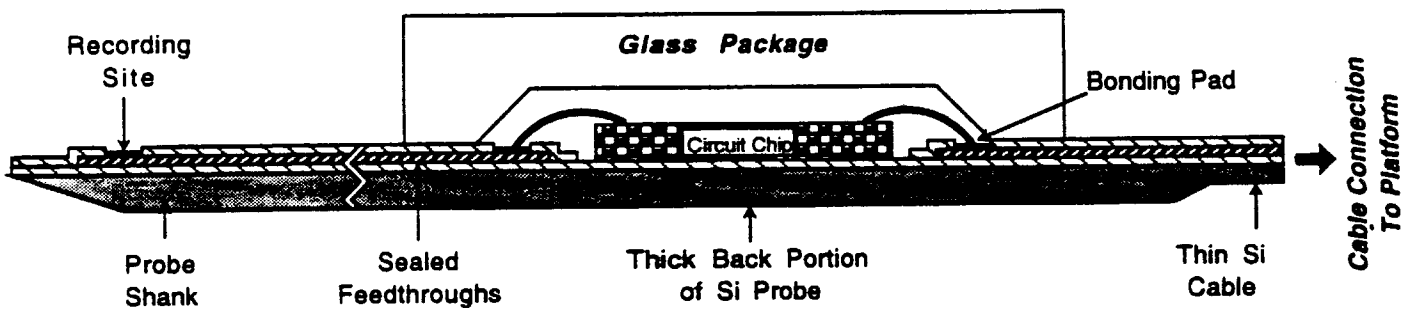

Figure 2: Proposed packaging approach for implantable neural prostheses that contain electronic circuitry, either monolithically fabricated in the probe substrate or hybrid attached to the silicon substrate containing microelectrodes.

2. ACTIVITIES DURING THE PAST QUARTER

2.1 Hermetic Packaging

Over the past few years we have developed a biocompatible hermetic package with high density multiple feedthroughs. This technology utilizes electrostatic bonding of a custom-made glass capsule to a silicon substrate to form a hermetically sealed cavity, as shown in Figure 3. Feedthrough lines are obtained by forming closely spaced polysilicon lines and planarizing them with LTO and PSG. The PSG is reflowed in steam at 1100°C for 2 hours to form a planarized surface. A passivation layer of oxide/nitride/oxide is then deposited on top to prevent direct exposure of PSG to moisture. A layer of fine-grain polysilicon (surface roughness 50Å rms) is deposited and doped to act as the bonding surface. Finally, a glass capsule is bonded to this top polysilicon layer by applying a voltage of 2000V between the two for 10 minutes at 320 to 340°C, a temperature compatible with most hybrid components. The glass capsule can be either custom molded from Corning code #7740 glass, or can be batch fabricated using ultrasonic micromachining of #7740 glass wafers.

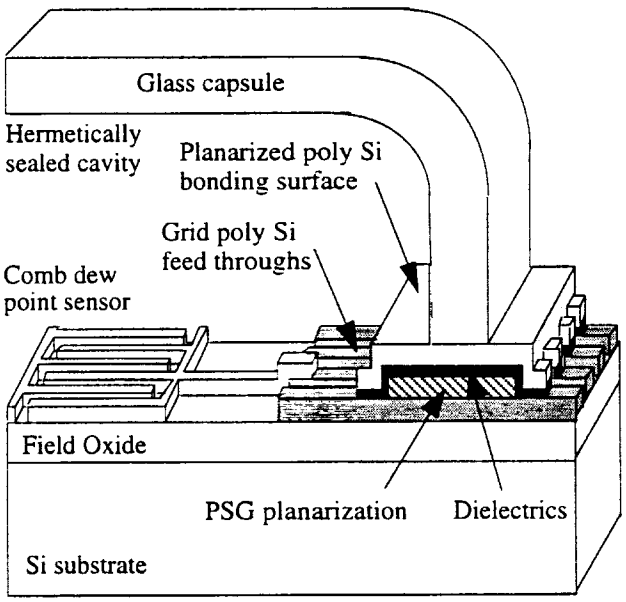

Figure 3: The structure of the hermetic package with grid feedthroughs.

During the past years we have electrostatically bonded and soak tested over one hundred and sixty of these packages. The bonding yield is about 82% (yield is defined as the percentage of packages which last more than 24 hours in the solution they are soaked in). We should also mention that the earlier tests that have been going for more than about 3 years (room temperature soak tests in saline and the 85°C and the 95°C tests in deionized water) have been made with silicon substrates that are thinned (~150μm) and bonded to the custom molded glass capsules. All of the relatively recent tests (85°C and 95°C tests in saline) are performed with the silicon substrates having full thickness (~500μm) and bonded to the ultrasonically machined glass capsules with a flat top surface. We currently have devices tested in deionized water for over 3.7 years at 85° C, and in saline at room temperature for over 3.4 years. A set of devices have been coated with a silicone coating and were soaked in saline during the 2 previous quarters. From this set of packages one sample is still under test after 283 days of soaking in saline at 85°C. The ongoing tests are detailed in the following sections.

2.1.1 Ongoing Accelerated Soak Tests in Deionized Water

We have continued our accelerated soak tests in deionized water. At the present time, out of the original 20 packages we have 2 packages that have lasted for more than three and a half years of testing time with no sign of moisture penetration inside them. In these tests temperature is chosen as the accelerating factor since it is easy to control and also the diffusion of moisture is a strong(exponential) function of temperature. We had started soaking 10 samples each at 85°C and 95°C. Tables 2 and 3 below list some pertinent data from these soak tests. Figure 4 summarizes the final results from the 95°C soak tests and figure 5 summarizes the results obtained so far from the 85°C tests. These figures also list the causes of failure for individual packages when it is known, and they show a curve fit to our lifetime data to illustrate the general trend. The curve fit, however, only approximates the actual package lifetimes since some of our packages failed due to breaking during testing rather than due to leakage.

At the beginning of this quarter, we had 2 packages soaking at 85°C. These packages are still dry and under test. For these packages we define failure as the room temperature condensation of moisture inside the package. The testing sequence for these packages start by cooling the sample to room temperature from its soak bath at the elevated temperature. The samples are next rinsed with deionized water and then dried with a nitrogen gun. We then measure the impedance of the dew point sensors and inspect the sample carefully for leakage under the microscope. The significant change in impedance (about 2 orders of magnitude) and observation of visible condensation inside the package would both be classified as the failure of the package under test.

Of the original 10 samples in the 95°C tests, the longest lasting package survived for a total of 484 days. The calculated mean time to failure of these packages are 135.7 days excluding the handling errors. Of the original 10 packages in the 85°C soak tests there are still 2 with no sign of room temperature condensation. The longest lasting package in the 85°C tests has lasted a total of 1347 days and is still under test. The mean time to failure for these tests has been calculated as 1026 days excluding the handling errors.

Table 2: Key data for 95°C soak tests in DI water.

Number of packages in this study	10
Soaking solution	DI water
Failed within 24 hours (not included in MTTF)	1
Packages lost due to mishandling	2
Longest lasting packages in this study	484 days
Packages still under tests with no measurable room temperature condensation inside	0
Average lifetime to date (MTTF) including losses due to mishandling	*118.7 days*
Average lifetime to date (MTTF) not including losses due to mishandling	*135.7 days*

Table 3: Key data for 85°C soak tests in DI water.

Number of packages in this study	10
Soaking solution	DI water
Failed within 24 hours (not included in MTTF)	2
Packages lost due to mishandling	3
Longest lasting packages so far in this study	1347 days
Packages still under tests with no measurable room temperature condensation inside	2
Average lifetime to date (MTTF) including losses due to mishandling	*652 days*
Average lifetime to date (MTTF) not including losses due to mishandling	*1026.4 days*

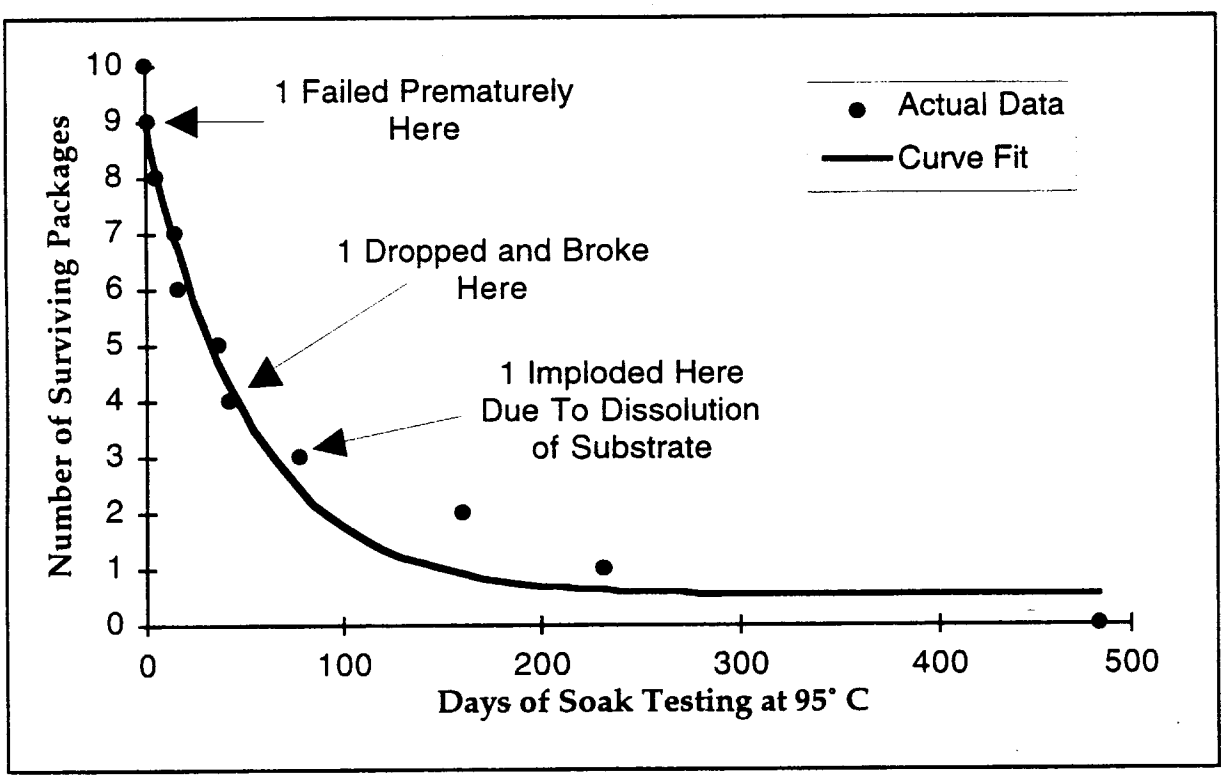

Figure 4: Summary of the lifetimes of the 10 packages which have been soak tested at 95°C in DI water.

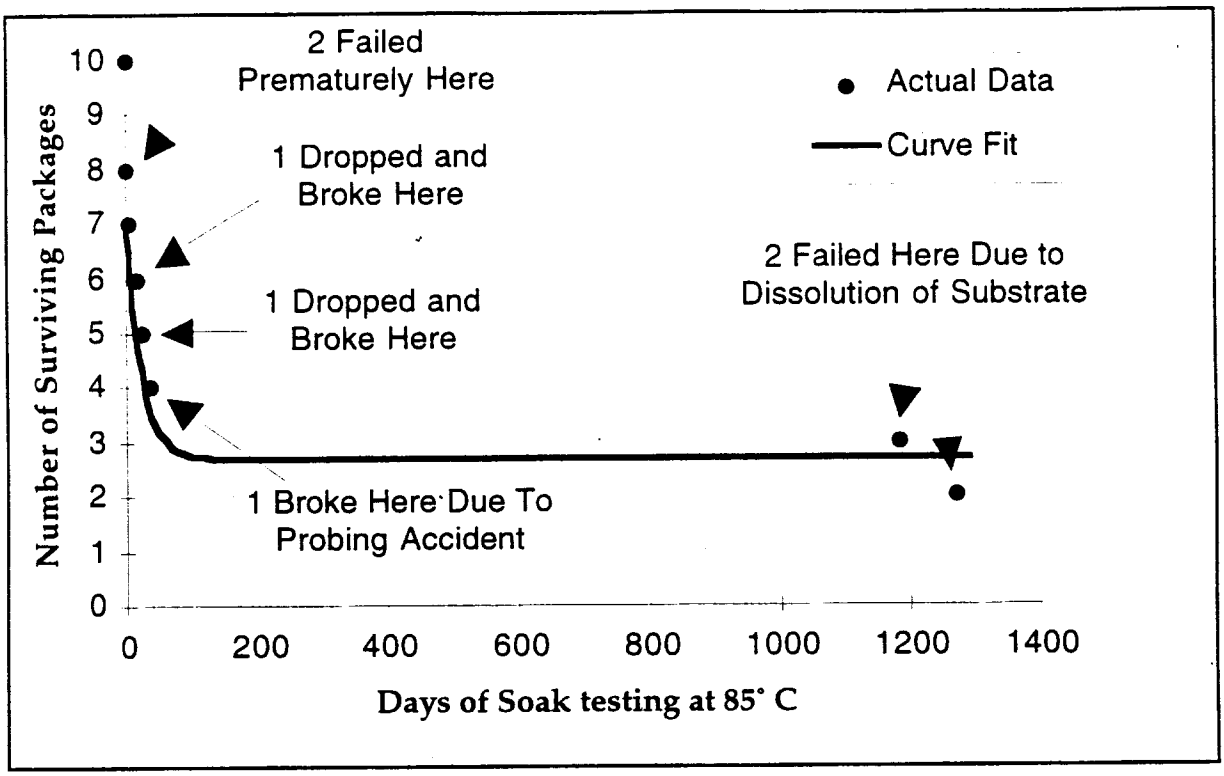

Figure 5: Summary of the lifetimes of the 10 packages which have been soak tested at 85°C in DI water.

2.1.2 Interpretation of Soak Test Results in Deionized Water

Generally during accelerated testing, one models the mean time to failure (MTTF) as an Arrhenius processes (In the VLSI industry this model is used for failure due to diffusion, corrosion, mechanical stress, electromigration, contact failure, dielectric breakdown, and mobile ion/surface inversion). The generalized equation used in all these cases is given below where MTTF is the mean time to failure, A is a constant, ξ is the stress factor other than temperature, (such as pressure or relative humidity), n is the stress dependence, Q is the activation energy, K_B is Boltzman's constant, and T is the temperature in Kelvin.

$$MTTF = A \cdot \xi^{-n} \cdot e^{\left(\frac{Q}{K_B T}\right)}$$

For the accelerated soak tests that we have performed on the packages, there was no stressing factor other than temperature, so the ξ term drops out of the above equation. The resulting equation can be rewritten as a ratio of MTTFs as it is below. This is the model we are using to interpret the accelerated soak tests performed during the past year.

$$AF = \frac{MTTF_{Normal}}{MTTF_{Accelerated}} = e^{\frac{Q}{K_B}\left(\frac{1}{T_{Normal}} - \frac{1}{T_{Accelerated}}\right)}$$

By using these MTTFs at 85°C and 95°C, we can easily calculate the activation energy (Q) and from this activation energy we can proceed to obtain an acceleration factor (AF) for these tests, and then calculate the MTTF at the body temperature. Moreover, after analyzing our failed samples we have found out and mentioned in the past progress reports that some of the samples at the 95°C tests have failed prematurely due to the enhanced dissolution rate for silicon at this temperature. Since the dissolution reaction is an exponential function of temperature, the samples at the 85°C tests have been effected less than the ones at 95°C. The model we use only accounts for acceleration of moisture diffusion, but not dissolution. We will still keep and update the data for the tests performed at 85°C. Moreover, for our calculations we assume that all the samples in the 85°C tests have also failed the same time as the longest going sample in the 95°C tests and proceed with the calculations as follows:

$$MTTF|_{85°C} = 257.6\,Days \quad MTTF|_{95°C} = 118.7\,Days$$

Q=0.88 eV, AF(95°C)=179.5, AF(85°C)=82.7

$$MTTF|_{37°C} = 58.4\,Years$$

We should also note that we have included every single sample in the 85°C and 95°C soak tests in this calculation except the 15% which failed during the first day (we assume that these early failures can be screened for). Moreover, some of these capsules have failed due to mishandling during testing rather than due to actual leakage into the package. If we disregard the samples that we have attributed failure due to mishandling we obtain a longer mean time to failure:

$$MTTF|_{85°C} = 396\,Days \quad MTTF|_{95°C} = 136\,Days$$

Q=1.217 eV, AF(95°C)=1304, AF(85°C)=447

$$MTTF|_{37°C} = 485\,Years$$

2.1.3 Accelerated Soak Tests in PBS Of Silicone-Coated Glass Silicon Packages

As described in the past contract reports, in order to slow down the dissolution of the top polysilicon layer (on the bonding surface of the device) we used a biocompatible silicone coating from Nusil technology which prevents the ions in the solution from reaching the bonding surface. Figure 6 shows a SEM view of our ultrasonically machined glass capsule/silicon package with a silicone rubber coating. As can be seen on this picture the coating material is applied on the interface between the glass capsule and the polysilicon bond. The coated devices have been soaking into saline for the last 3 quarters at high temperature. Using our acceleration models, we have been able to obtain a predicted lifetime of the packages at body temperature.

We started our tests with 8 devices at 85°C and 8 devices at 95°C. Out of the original 8 packages at the 85°C tests, one of them failed after one day (premature failure) due to a fault on the bonding surface. This device was not included in our calculations. During the last quarter, 6 out

of the 7 remaining packages have failed. The first device failed after 138 days and one package is still dry after being soaked for 283 days. Table 4 and Figure 7 give an update and summarize the obtained results, and the failure mechanisms are described in the next section. Assuming that the remaining device failed at the time of writing this report, we would calculate a Mean Time To Failure (MTTF) of 212 days for the devices soaking at 85°C.

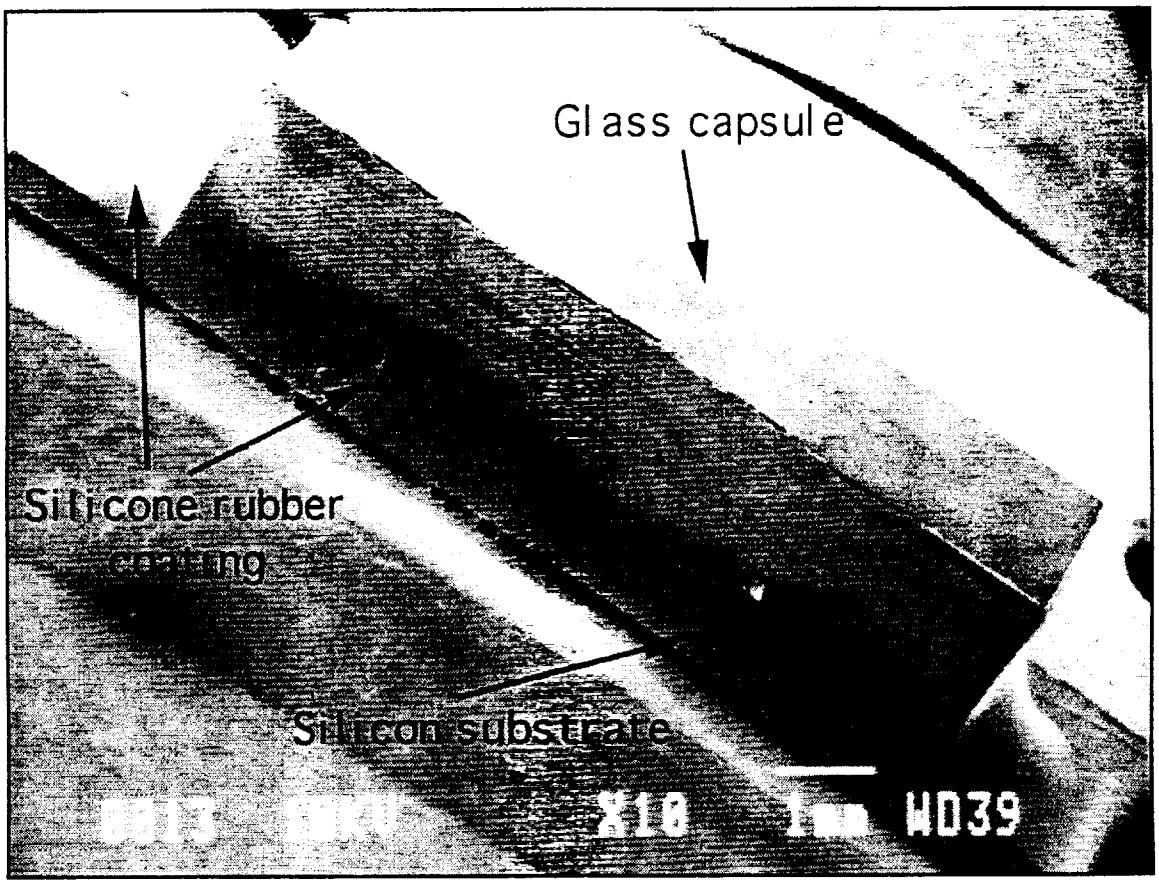

Figure 6: SEM of a silicone-coated glass-silicon package.

Table 4: Key data for soak tests in saline at 85°C.

Number of packages in this study	8
Soaking solution	Saline
Failed within 24 hours (not included in MTTF)	1
Longest lasting packages in this study	283 days
Packages still under tests with no measurable room temperature condensation inside	1
Average lifetime to date (MTTF)	*212 days*

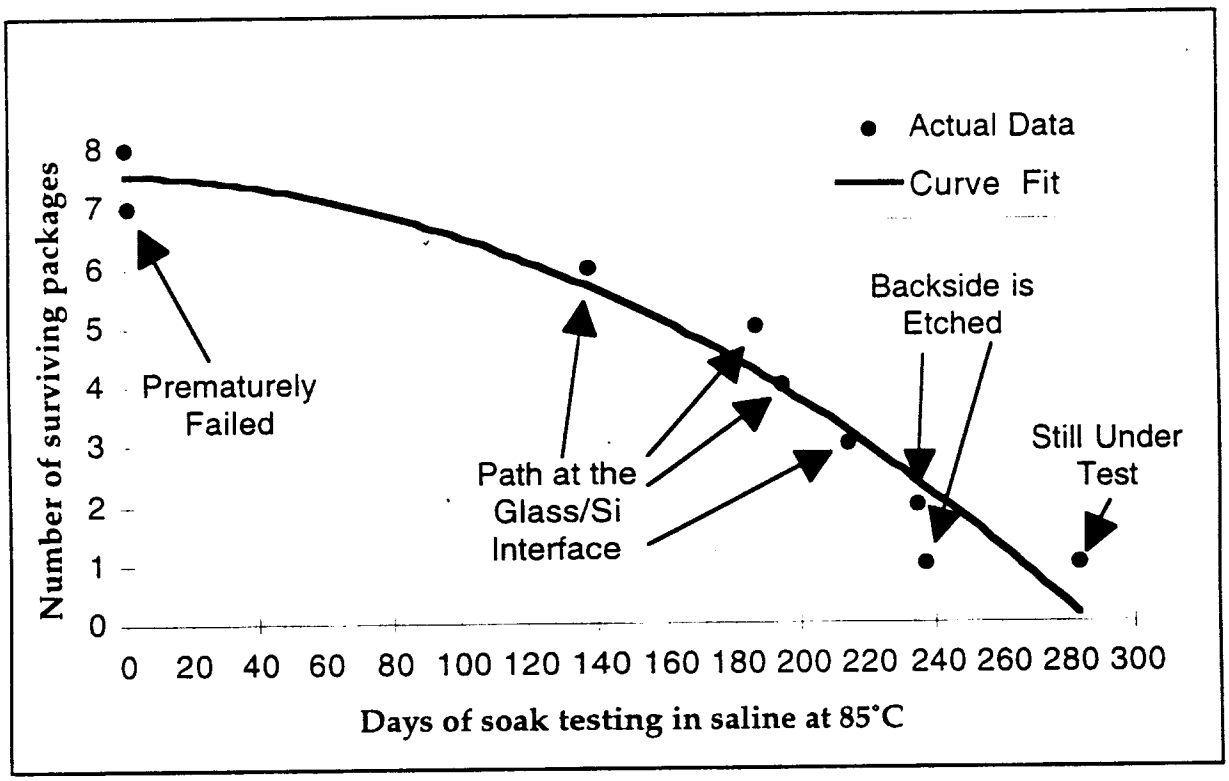

Figure 7: Summary of the lifetime of the 8 packages soaked in saline at 85°C.

Out of the 8 packages soaked at 95°C, one failed after the first day because of a scratch on the polysilicon bonding surface. This package was not included in our calculations. Out of the 7 remaining packages, the first failed after 70 days, the longest lasting package failed after 203 days and we calculate a MTTF of 125 days. Table 5 and Figure 8 give an update and summarize the obtained results.

During those tests, the packages were monitored every few days for room temperature condensation both electrically by means of an integrated dew point sensor (when probing was still possible) and also visually by the aid of a microscope. With these ultrasonically machined glass capsules, due to their flat top surface, we have the additional advantage of being able to monitor their bonding surface and the glass capsule to polysilicon interface for discoloration and dissolution. When electrical testing of the dew point sensors is possible the failure is defined as condensation at room temperature (the devices are cooled down to room temperature before testing).

Table 5: Key data for soak tests in saline at 95°C.

Number of packages in this study	8
Soaking solution	Saline
Failed within 24 hours (not included in MTTF)	1
Longest lasting packages in this study	203 days
Packages still under tests with no measurable room temperature condensation inside	0
Average lifetime to date (MTTF)	*125 days*

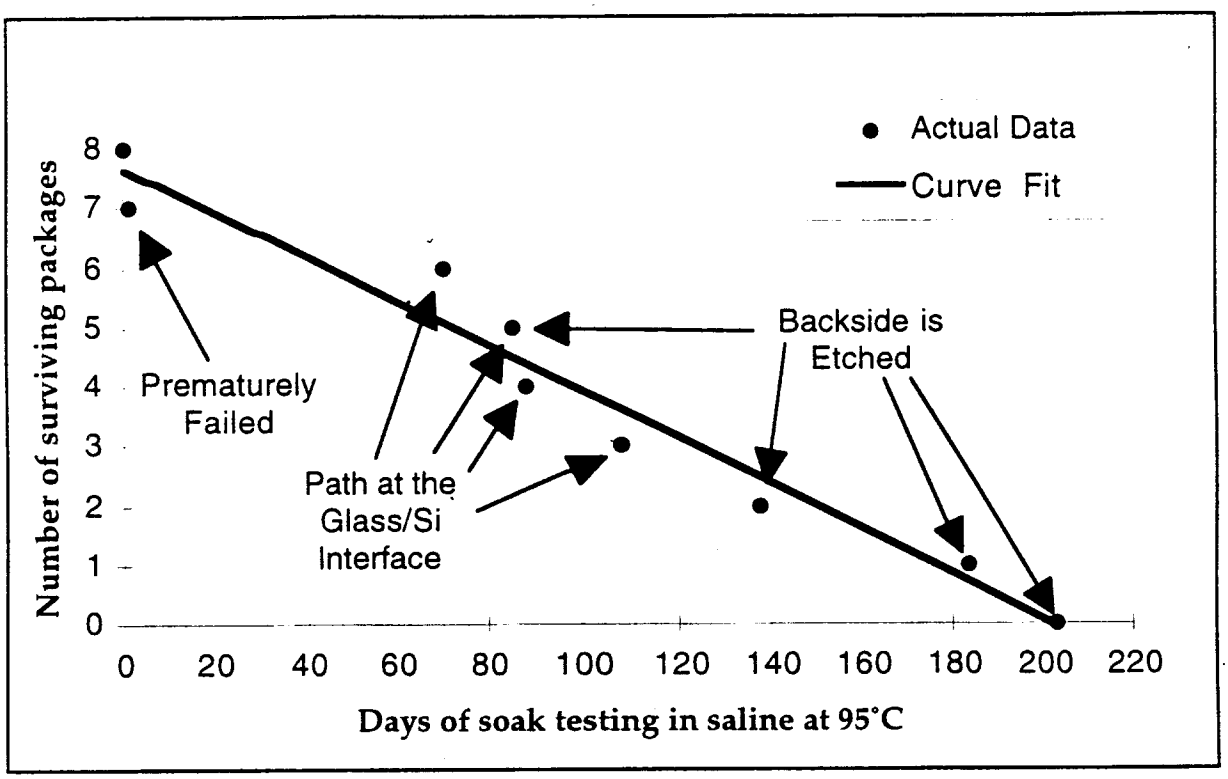

Figure 8: Summary of the lifetime of the 8 packages soaked in saline at 95° C.

The condition of the packages during the soaking period was as follows. First, some dissolution is observed around the edges of the devices. After some time, if the inside of the package is still dry, the dissolution of the probing pads eventually prevents electrical testing (by impedance measurement of the dew point sensors) of the sensors inside the devices. However, a visual observation using a microscope allows scanning through the glass capsule for leakage paths on the polysilicon bonding region, and water is also observed inside the package if a path is created through the substrate itself. The device is claimed failed once a path through the bonding surface or some water inside the package have been observed. In order to overcome the limitations due to the dissolution of the probing pads, we are currently working on developing some telemetry techniques used to monitor dew point and humidity inside the packages. Those techniques are described in some later sections of this report.

If we compare the average lifetime of the packages obtained at high temperature in these tests with the previous results obtained with the uncoated devices, we can see a significant improvement due to the silicone rubber coating: this is quantitatively illustrated in Table 6. For the uncoated devices soaked at 95°C, we had a MTTF of 38 days and the longest lasting package had failed after only 70 days. Thus, the silicone coating effectively prevents the corrosion of the top polysilicon layer. This seems to be confirmed by the fact that in the tests of the uncoated devices, the top polysilicon dissolution was the main failure mechanism. In current tests of the coated devices we have observed some failures due to the etching of the substrate itself. As we will see in the following section concerning the failure modes, we also believe that this coating would be efficient in slowing down the etching of the silicon substrate itself, when applied on the sidewalls of the substrate. Using the MTTF obtained at 85°C and 95°C, and the acceleration model described in the previous section, we can calculate a predicted Mean Time To Failure at body temperature of 11.8 years.

Table 6: Comparisons of the coated and the uncoated packages in saline.

		Coated packages (current tests)	Uncoated packages (past tests)
85°C	Shortest lasting package	138 days	15 days
	Longest lasting package	283 days (still under test)	321 days
	MTTF	212 days	115.6 days
95°C	Shortest lasting package	70 days	10 days
	Longest lasting package	203 days	70 days
	MTTF	125 days	38 days
Predicted MTTF at body temperature		11.8 years	117 years

Some important remarks should be made when comparing the results obtained with the coated and the uncoated devices. First, as far as the coated devices are concerned, one device is still under test, and the results will have to be updated when the study concludes. Second, the number of uncoated packages under test was different: 17 packages were soaked at 85°C and 11 were soaked at 95°C. Last but not least, the predicted Mean Time To Failure (MTTF) at body temperature for the coated devices is probably underestimated, because our acceleration model does not take into account the fact that many mechanisms, and not a single one, are responsible for the failures of the devices. Indeed, we observe a significant improvement in the lifetime of the packages when a coating is applied, which should result in an improvement in the lifetime of the packages at body temperature, which is not what is obtained when deriving the MTTF at 37°C when using our acceleration modeling. We are currently working on the issue of our acceleration modeling.

2.1.4 Failure Modes

The devices in these tests have been checked for moisture penetration every few days both with the dew point sensors and also visually with the aid of a microscope. The possible failure mechanisms are illustrated in Figure 9 below.

Two main failure modes have been identified during the past quarters. One of them is attributed to the dissolution of a polysilicon layer just below the glass capsule. The dissolution of the polysilicon layer eventually creates a path, a typical one of which can be seen on Figure 10(a). The Figure 10(b) shows the way the picture is taken from the top.

Another possible failure mode has been identified, which is the dissolution from the backside of the silicon substrate. Figure 11(a) shows a picture of the backside of the device etched to the point that we can see the inside of the package (region A shows dissolution of the backside of the substrate and of the glass/silicon interface, region B shows dissolution of the backside of the substrate only and region C shows the remaining non etched layers). Figure 11(b) shows the way the picture is taken from the top.

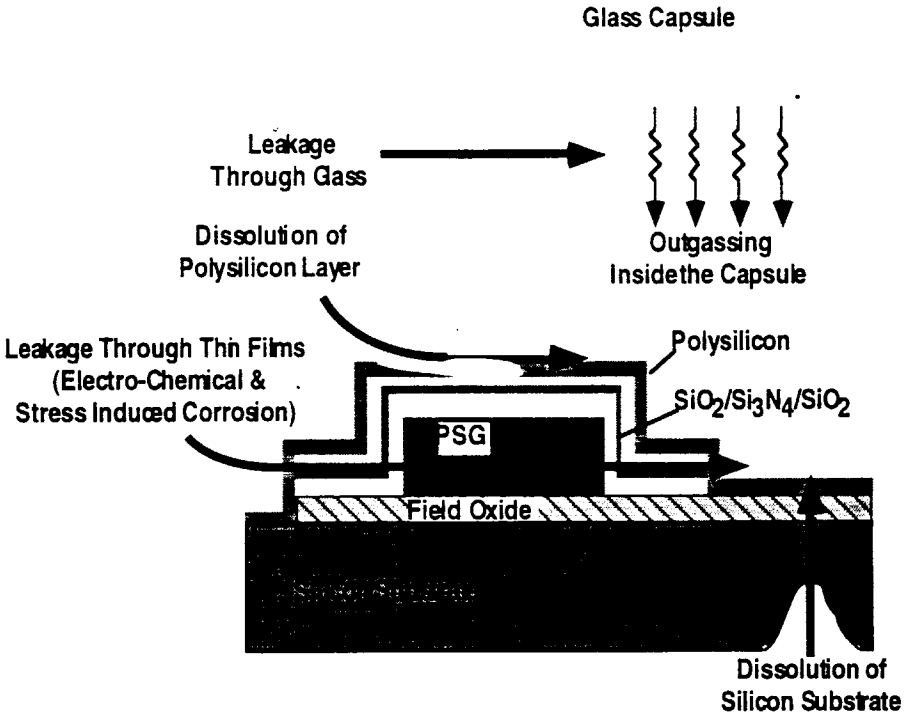

Figure 9: The possible failure modes for the microstimulator package.

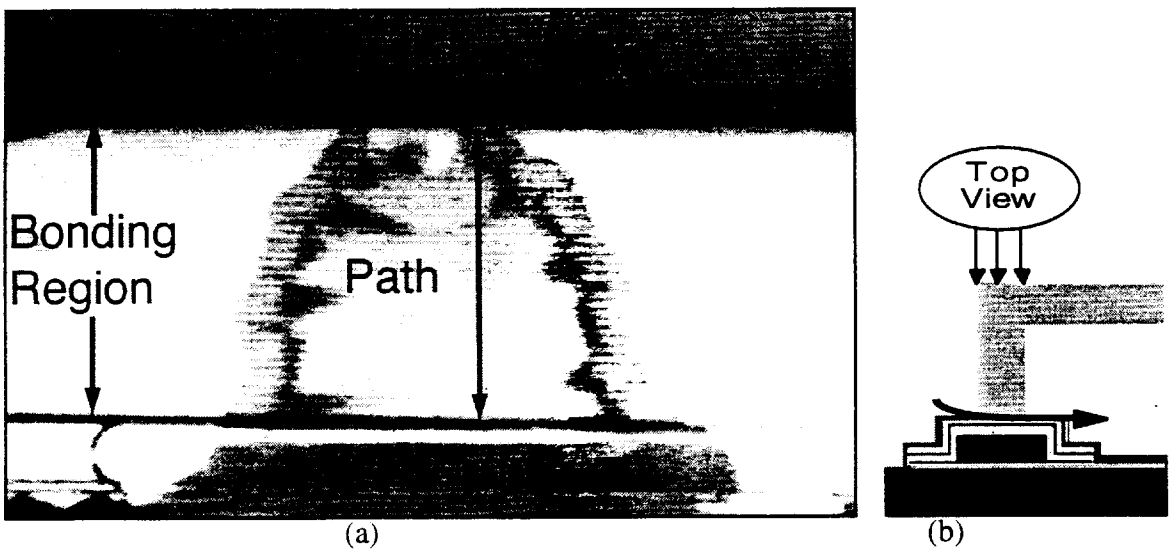

Figure 10: Leakage path through the interface between glass and silicon seen from top after soaking for 88 days at 95°C.

(a) (b)

Figure 11: Backside view of the device.

In order to attempt to identify the mechanism behind the dissolution of the silicon substrate, we performed surface analysis (by the use of an X-ray detector mounted on a SEM) of the backside of a device which had been soaking for almost 200 days at 95°C. Although no significant result was obtained from the chemical analysis, some SEM pictures such as the one shown on Figure 12 show the result of the dissolution of the backside of the silicon substrate. In Figure 12, we can see the crystalline structure of the silicon after a film is peeling off the backside of the substrate.

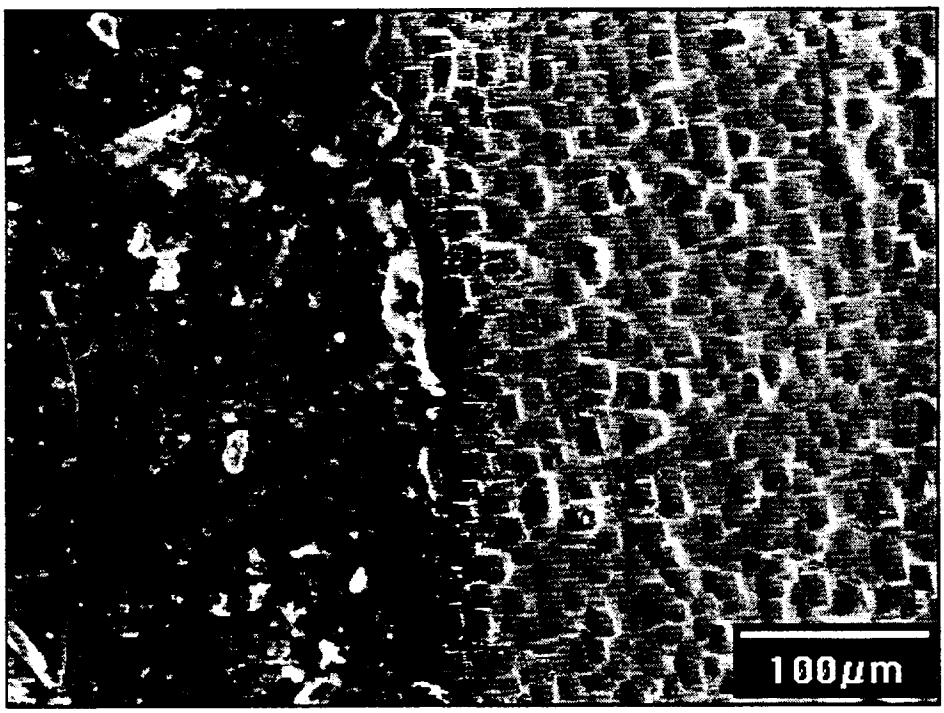

Figure 12: SEM of the backside of the substrate after soaking 200 days at 95°C.

As we saw in the previous section when comparing the results obtained for the coated and the uncoated devices, the silicone coating has been effective in slowing down the dissolution of the top polysilicon layer (corresponding to the first failure mode described above). It seems that the

coating is also effective at slowing down the dissolution of the substrate. Indeed, from visual observation it seems that the solution attacks the silicon substrate on the vertical sidewall of the silicon substrate, creating an arch-shaped etching (illustrated on Figure 13).

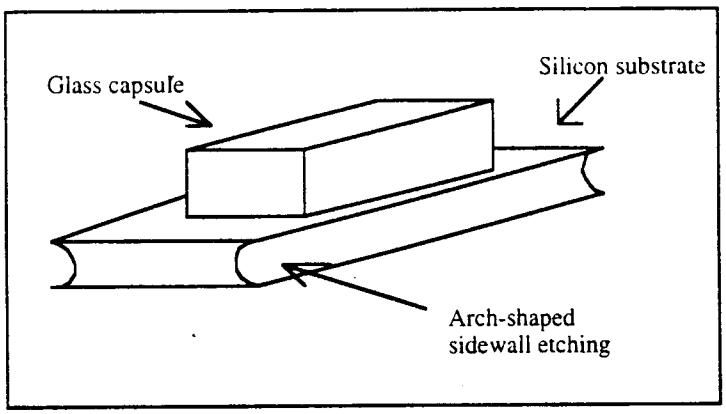

Figure 13: Arch-shaped etching of the substrate.

If the coating, when applied on the interface silicon/glass, overlaps one edge of the silicon substrate, it seems that the substrate dissolution is also slowed down, as can be seen in Figures 14 and 15, showing a picture of the device which is still dry after being soaked for 283 days at 85°C. On this picture we can see that where the silicone coating overlaps, the dissolution of the substrate is less advanced than on the two ends of the substrate where there is no protective coating.

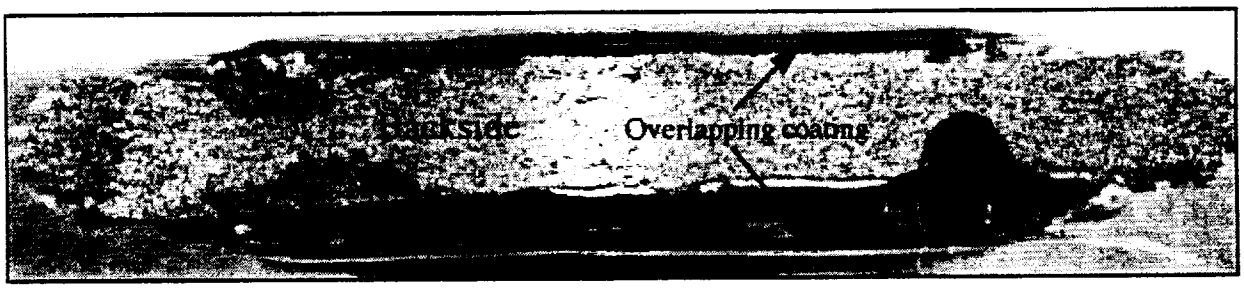

Figure 14: Backside view of a coated device after 283 days in saline at 85°C.

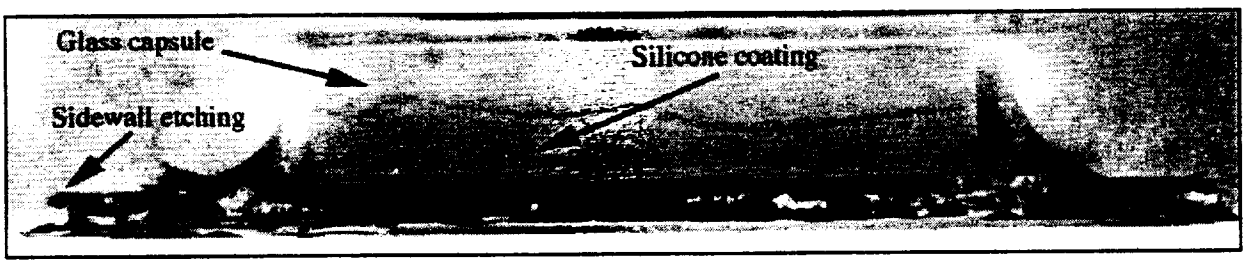

Figure 15: Side view of a coated device after 283 days in saline at 85°C.

2.1.5 Ongoing Room Temperature Soak Tests in Saline

We have continued the soak tests with the glass capsules bonded to Silicon at room temperature in phosphate buffered saline solution. Table 7 below summarizes the pertinent data from these soak tests. We have originally started these soak tests to complement the accelerated soak tests at the higher temperatures. We have consistently observed in these tests that at room temperature we are below the activation energy required to cause dissolution and hence we have not yet observed any dissolution related failures.

We have soaked 6 packages in phosphate buffered saline at room temperature. One of these packages leaked within a day, indicating surface defects or poor alignment of the glass capsule to the silicon substrate. Another one failed after 160 days of soaking. This failure was attributed to mishandling. The longest lasting package has survived a total of 1247 days and is still under test. The remaining 4 packages have shown no sign of moisture either measured electrically or observed visually after an average of 1022 days of soaking (if we include the one device whose loss is attributed to mishandling) and 1242 days if we do not include the device failed because of mishandling. Those 4 packages are still under test.

Table 7: Data for room temperature soak tests in saline.

Number of packages in this study	6
Soaking solution	Saline
Failed within 24 hours (not included in MTTF)	1
Packages lost due to mishandling	1
Longest lasting packages in this study	1247 days
Packages still under tests with no measurable room temperature condensation inside	4
Average lifetime to date (MTTF) so far including losses due to mishandling	*1022.4 days*
Average lifetime to date (MTTF) so far not including losses due to mishandling	*1242 days*

2.2 Preventing Dissolution of Silicon In Accelerated Testing

2.2.1 Problem Statement

As mentioned previously, the failed devices in the accelerated saline soak tests have been carefully examined in order to find the causes of failure. The conclusion is that the silicon both in single crystalline form and also in polycrystalline form at these elevated temperatures is prone to dissolution. In parallel with these tests we have conducted implant studies both here and Vanderbilt University and also in Hines VA Hospital in Chicago. We have carefully examined the packages implanted here and also in VA Hospital. In both of these sets of implants we have not observed the dissolution of silicon or polysilicon after 2 months of implantation which suggests that the dissolution at the body temperature is very negligible. We will do a series of tests in the future to characterize the exact temperature of this dissolution mechanism and find its activation energy, but for the present we would like to look into an alternative solution so that we can continue our soak tests. This section will emphasize the plan of action to resolve the dissolution problem. In summary, the dissolution mechanism is causing 2 main problems in our tests which are :

(1) Dissolution of the bonding polysilicon layer below the glass capsule.
(2) Dissolution of the silicon substrate.

We should also note that the oxide and nitride layers that are exposed to the saline solution at these elevated temperatures have been found to be very stable and as such do not show any measureable signs of dissolution and hence do not cause device failures.

2.2.1 Preliminary Work For Elimination Of This Failure Mode

During the past year, in order to continue our accelerated soak tests in saline we have tried to stop this dissolution by coating the polysilicon glass interface with a biocompatible Nusil silicone coating and have found that this coating increased the MTTFs by a factor of about 3. The coating is effective for some time, but over time the saline solution erodes the coating and eventually reaches the interface and causes dissolution. Moreover, the silicon substrate gets also attacked in saline which is one of main reasons for device failure. Our conclusion is that the silicone coating wears away with time and thus is only a temporary solution. A more permanent solution is being investigated.

2.2.2 The Solutions To Overcome The Dissolution Problem

There are several approaches for resolving the dissolution problem of silicon in saline. Our main goal is to be able to test our devices under accelerated conditions corresponding to their actual environment. As such, even though the de-ionized water solution does not attack silicon we are not considering using de-ionized water since it is not the best environment that is a replica of the body environment. Hence even though the saline environment is giving us additional problems it is the environment that is used by most researchers for in-vitro studies. Another option is to use lower temperatures, but this solution is also not very feasible due the extent of the duration of the accelerated tests. We would like to point out that since the glass silicon bond is a hermetic bond, the coating or the solution need not have to be barrier against moisture and the main goal behind the coating is to be able to act as a barrier against the ions in the saline solution so that we can continue our accelerated tests. In general we can classify the solution groups into 3 main categories which are detailed in the following sections and are (i) Coatings, (ii) Electrochemical bias, (iii) Design Changes. Before going into detail in each of these subsections, we will summarize below the requirements of this solution to overcome the dissolution of silicon in saline at high temperatures:

1) Biocompatible
2) Low temperature process ($T < 400°C$)
3) Transparent to RF
4) Inexpensive and fast turn around time
5) Should be thick enough to seal the glass silicon interface of 5 microns
6) Should act as a barrier against the ions in saline

The main requirement for the solution is that since it will be eventually used inside a living organism, it has to be biocompatible. Most of the hybrid components in the microstimulator get damaged after reaching temperatures higher than 400°C and as such the deposition temperature of the coating or the metal has to be below this temperature. Most of the metals that can be used as coatings are also a feasible solution since we need to transfer power and data to the coil inside the package which is impossible in case of metals. Since we are testing many components at a time we prefer the solution to be affordable with a fast turn around time to continue our studies. After the assembly process we also expect this coating step to be compatible with batch processing and simple enough to allow us to prepare many devices preferably with a high yield.

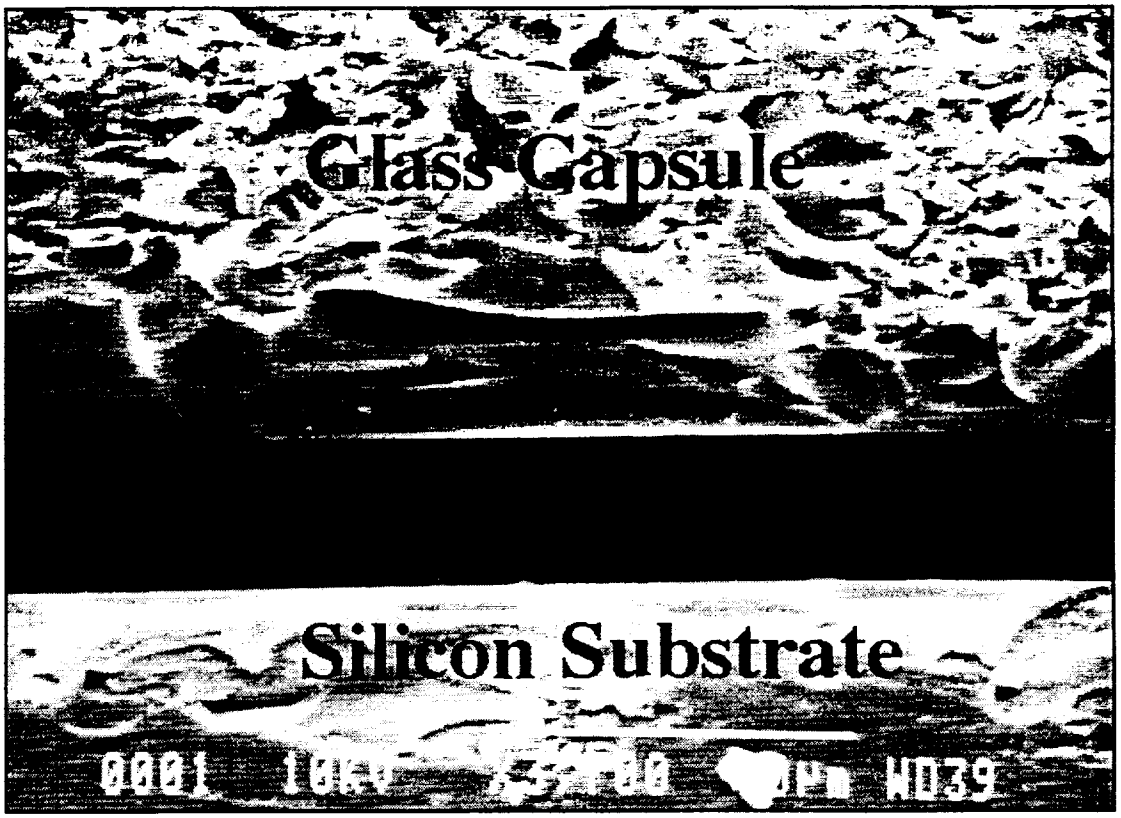

Figure 16: The gap between the silicon substrate and the glass capsule.

As seen in Figure 16, the glass capsule sits over the silicon substrate by a distance of 5μm. Hence, the coating either has to seal this interface or has to penetrate underneath the glass capsule and coat the walls conformally so that none of the polysilicon layer is exposed to the saline solution. Moreover, we also expect it to be thin so that it does not make the final device unacceptably large. Since we will be using the electrode sites for stimulation of the tissue we need to have the electrodes exposed to the body solution which requires that we also have to find an effective masking method for the electrodes from the materials we are depositing onto the package. A final requirement is that it should act as a barrier for the ions in the solution whereas it can be transparent to moisture. With this we will detail the possibilities for each category of solutions. We should also add that this list is not a complete list, but kept to a minimum due to the fact that we want to minimize the fabrication time by using a solution available to us in our laboratory or university.

(i) Coatings

There are various coatings available for sealing the device such that the silicon layers are not exposed to the saline solution. Some possibilities are:

UM Solid State Laboratory

PECVD oxide/nitride layers

Paralyne C
Teflon
Polyimide
Biocompatible Epoxy
Nusil Silicone
A combination of any of the layers above

UM Other Departments

Prof. Martin (MatSci) Biocompatible fiber coatings
Prof. Burns (ChemE) Self assembled monolayers

(ii) Electrochemical Bias

An electrochemical bias on the silicon layer with a metal can stop silicon etching. As such we can bias the silicon with an electrode painted to the silicon layers, or better yet could attach a metal to the silicon which will generate the correct bias between the silicon and the solution and hence stop the dissolution. The general solution is the application of an electrochemical bias with the use of a metal. We are currently in the process of looking for the exact dissolution reaction. We are also trying to find the half cell potentials between the different metals (that we can deposit in our laboratory) and silicon in a saline solution. After the conclusion of this study we will perform some experiments with the metals in our lab to test their effectiveness and will incorporate them into our next package design.

(iii) Design Changes

A final solution is to make some design changes to the materials used in the fabrication of the silicon glass package. Before doing experiments we will study the theory behind the silicon etching process and then design experiments with individual pieces to see the effectiveness of the solution. Not deglazing the top polysilicon layer after its doping is one of the possible solutions. We have observed in our tests that the oxide layer is fairly stable even for long periods in elevated temperatures in saline. Hence, after doping the second polysilicon layer, we will typically get a layer of Phosphorus rich oxide. We used to etch this oxide layer to be able to bond to the top polysilicon layer. Our experiments have shown that one can also bond through thin oxide layers and hence we do not need to etch this top oxide layer. This solution may stop the dissolution of polysilicon however since the oxide is not known to be a good barrier for moisture, this particular solution requires an additional coating to stop moisture penetrating into the package through this oxide layer on top of the polysilicon. Moreover, this method would only protect the bonding poly and not the silicon substrate which will be exposed after dicing individual pieces and this issue needs further consideration. We can use PECVD oxide after dicing to cover the lateral sides of the silicon substrate. A final BHF dip is required to open the probing pads for testing later on.

Using different dopants for the top polysilicon layer is another possible solution. In the past, we have only used Phosphorus for doping the top polysilicon layer. We also have Boron available to us in the laboratory and other dopants that we can use by ion implantation from outside vendors. This idea is similar to biasing the silicon surface to a level where it would be hard to cause dissolution. If we can dope the second polysilicon with a heavy dose of Boron this would likely stop the dissolution. We have looked at Boron doping and the effects of doping on the surface morphology and have not seen any significant changes compared with our current process when we use Phosphorus. Further issues include using a high dose of Phosphorus that can bring the Fermi level to a point so that the dissolution does not start. This particular solution does not solve the problem of the dissolution of the substrate which should also be considered.

Other surface treatments include passivation by oxidation and surface assembled monolayers to protect the silicon surface. We have already tried to place a substrate (with no glass capsule) into diluted HNO_3 solution to create a thin layer of oxide on top of the silicon, but the thickness of this oxide layer was not sufficient to stop the dissolution of silicon in saline. We have also looked at using surface assembled monolayers, however most of these are either too thin to be useful or are not effective after being exposed to the temperature of the anodic bonding step. We are looking into other possible solutions for the problem.

2.2.3 The Testing Procedure For The Proposed Solutions

To speed up the process of finding a solution we will try a few samples of each solution at the highest of the two elevated temperatures (95°C) and based on the success we will proceed with the actual tests. We have recently bought new ovens with better accuracy which we hope to utilize in our new both trial and also actual soak tests. We are also considering using the new autoclave for aging studies which will be used for short term reliability study of coatings. We expect to finish the trial tests for stopping the dissolution in the coming quarter and will continue with actual tests after that.

2.3 Accelerated Testing Of Implantable Devices

2.3.1 Introduction

During the past quarter, we further studied and performed a more complete literature survey about the various testing methods and models for accelerated testing of implantable devices. This section will detail some of the findings. Implantable prosthetic devices have progressed from simple wire electrodes to sophisticated electronic packages used to collect data from the body (pressure sensors, blood flowmeters, evoked potentials measurements) or to restore partial functions to damaged organs (cardiac pacemakers, muscle stimulators, neural stimulators). The growth in prosthetic device complexity emphasized the issue of packaging of implantable devices which has been an extremely complicated problem [1]. The packaging materials not only have to protect the circuitry from the hostile environments of the body, but also should be chemically stable and should have low toxicity and be hermetic for long periods of time. The fact that the implanted devices reside inside the living tissue makes it far more important that the package used to encapsulate them be highly reliable. It is equally important to know how long an implanted device can be expected to last while it is implanted inside a living organism. The implanted devices should be tested in a laboratory under conditions which simulate actual use. But the exact reproduction of implanted conditions is hard to accomplish. As such, accelerated tests need to be designed and the accelerated models need to be verified to estimate the lifetime of implanted devices under normal operating conditions.

2.3.2 Accelerated Testing

The term accelerated testing means acceleration of the normal time-to-failure process through the use of elevated stress. Accelerated testing is intended to shorten the normal time-to-failure process (which could take years) without changing the physics of failure. Accelerated tests can be broken down to include elephant tests and accelerated life tests. An elephant test usually consists of a single severe level of stress that is used to either reveal failure modes, give engineers confidence that a product is reliable or establish a pass/fail criteria. Accelerated life tests, on the

other hand, are used to estimate reliability, or life, by conducting tests at increased levels of stress. In this part we will focus on accelerated life tests.

As is well known [2]: "Acceleration tests are only valid if the mechanism that causes the failures is precisely the same as that observed in the real world". For this reason, prior to an accelerated test all the possible failure modes for the device need to be well known. Hence in the section below we will describe the failure modes obtained from the Glass-Silicon packages via in-vivo and in-vitro tests conducted over the past several years.

2.3.3 Device Failure Modes

Over the past 3 years we have performed in-vivo studies on more than 30 samples with the Glass-Silicon packages in several Medical Centers including University of Michigan, Vanderbilt University and Hines VA Hospital. The explanted devices are carefully inspected for dominant failure modes and in most cases the glass silicon package found to be intact and hermetic over the duration of the implant. In several cases, the failures resulted from an incomplete glass to silicon bond for reasons such as trapping of particles between the glass and the silicon bonding surface or misalignment between the glass and silicon surfaces. In other instances, the tissue of the living organism (bone or muscle) have grown over the implanted device and the device is broken during the explant operation. In summary, not many devices have failed during our in-vivo studies which means more implants are necessary for understanding the actual failure mechanisms which occur under the intended operational environment of our device.

During our in-vitro accelerated tests both in deionized water and in saline at elevated temperatures, we have observed the dissolution of both silicon and polysilicon layers to be the predominant failure mechanism. Using a silicone rubber coating has hindered this dissolution mechanism so that the mean time to failures have increased by about 3 times, but eventually the dissolution mechanism is the main cause of failures. The silicone rubber which is permeable to moisture slowed down the transfer of ions (Chlorine especially) and hence resulted in a longer lifetime. Moreover, the silicone rubber has a limited lifetime, due to adhesion loss and degradation from temperature cycling and also the swelling of the trapped air bubbles inside the coating, and eventually eroded exposing the silicon layers to the saline solution. We should also mention that one can use other implantable coatings, including paralyne C, Silicon nitride, polyimide and evaporated glass [3] with the main requirements of providing a barrier for the ions and also having good adhesion to the layers below (silicon and glass) which are detailed in a previous section of this progress report. It should also be mentioned that the silicone coating was not necessarily applied very uniformly in our tests and was simply a means of checking whether it would help reduce dissolution. A more careful application of the silicone is expected to significantly increase the MTTF beyond what we measured.

2.3.4 Design Of An Accelerated Life Test

There are government standards that give suggestions on how to run similar accelerated tests [4]. In summary, the following measures have to be carefully followed:

a. The pH value of the immersion fluid shall be maintained at 7.4±0.2 to simulate the in-vivo environment.
b. Before choosing an elevated temperature, the material system should be tested over a temperature range of 37 to 120°C. The purpose of this test is to determine if a material transition temperature (melting temperature) or a degradation temperature occurs within this temperature range. If a transition or degradation temperature is found between 37 and 120°C, then the maximum acceleration temperature to be used should be at least 25°C below the lowest

transition or decomposition temperature. If a transition temperature is not found then the accelerated tests can be conducted at T_a= 95°C.

c. After the completion of b, at least 5 samples representative of the specimen being evaluated should be tested each at both T_a and 37°C and then tested for temperature induced differences. in the case the temperature enhancement (except diffusion) has generated new properties in the specimens, then a lower temperature must be identified by repeating the procedure at selected lower temperatures.

Assuming an activation energy based model, one can determine the minimum number of stress levels to be included in the tests [5]. The data is plotted as the logarithm of the degradation rate versus reciprocal stress level (i.e., temperature), and a straight line is expected if only one degradation mechanism is occurring. Therefore. 3 stress levels should be sufficient to validate the straight line. However, to extrapolate to normal use conditions, one must be certain that a change in mechanism has not occurred. If two degradation mechanisms operate over the stress levels of the accelerated test, a minimum of five stress levels is required to define both straight lines. As such, a minimal test matrix should consist of:

1. 5 devices at each stress level.
2. Seven measurements over the period of the test.
3. Five levels of stress.

Moreover, the devices under test should be as identical as possible. There are 2 main approaches for modeling accelerated tests. There are several empirical life-relationship models that are used to extrapolate from accelerated conditions to usage conditions based on the stress levels and constants. With few exceptions, these models are empirical and based on curve-fitting of the data, and not on the physics behind the failure. These models have been used for accelerated testing everything from electronics to cables. Various references [6] state that failure mechanism models should be based on the physics behind the failure rather than testing. These models relate key parameters that are known to affect the reliability of the component and include the stresses on the component. This is the approach that we will be taking as the physics of failure for the devices are detailed below. Moreover, there may be times where a failure-mechanism model may not exist and an empirical model can be used. A later section mentions some of these models that are used in the broad accelerated testing literature.

2.3.5 Physics of Failure Approach to Modeling

Physics of failure is an approach to design, reliability assessment, screening that uses knowledge of rootless failure processes to prevent product failures through robust design and manufacturing practices. This involves identifying potential failure mechanisms, identifying the appropriate failure-mechanism models and their input parameters, determining the variability for each design parameter and computing the reliability function, mean and the median. From a physics of failure approach to modeling lifetime of the glass-silicon package, we noticed 2 different factors that cause the failure of the package. The first one is the erosion of the coating and the second is the dissolution of the silicon layers. The erosion of the coating can be studied by using a substrate and use of different biocompatible coatings. The adhesion of silicone rubber to several materials are studied [7,8,9] and understood. One should also be careful while calculating the mean time to failures so that they include only the samples failed from the mode under consideration. For instance, while calculating an activation energy for our failures in deionized water, we should exclude all the samples that were dropped from the calculations since these would not be failures that lead to the calculation of a unique activation energy. Moreover, when there are 2 different failure mechanisms, the assumption and the estimation of a single activation energy cannot be used. For instance, for the calculations done on the coated devices, since there are 2 mechanisms for the moisture to penetrate, one should try to find activation energies related to

both. This may include dividing the failed samples into 2 groups, one being failures caused from the erosion of the silicone rubber and then the dissolution of the polysilicon layer and the other group of samples that have failed from only the dissolution of the silicon substrate. As mentioned before, the failure mode should be a representative of an actual failure mode under normal operating conditions which should be verified with the in-vivo studies. We can also perform the dissolution experiments at 5 different temperatures with bare silicon substrates to determine the dissolution rate at each temperature with the suggestions mentioned above. A third failure which has never been observed is the diffusion of moisture along the interface between glass and silicon. There are models derived in the literature that include the effect of pressure gradient to model moisture diffusion along the cracks of the interface along with acceleration factors, however we never have observed this failure mode because the premature dissolution of the polysilicon (which is not expected to be significant at body temperature) prevents the observation of these other failure modes. Moreover, when a bond is formed around a dust particle the size of the unbonded region is different in each case. Furthermore, there are photolithographic faults which generate unbonded regions with different randomly distributed dimensions.

2.3.6 Acceleration Mechanisms

Often the reliability requirements depend on the application environment of the final devices. For example, if a product is to be used in a ground application in tropical areas, then humidity related areas will be considered to be most likely and the appropriate data for qualification must be derived from accelerated humidity testing or combined temperature and humidity. If the same product is to be used in a space satellite with a low earth orbit, humidity is not an issue but radiation dose and dose rate should be used. With this introduction, we will detail some of the mechanisms that can be used for accelerating moisture diffusion into the hermetically sealed implantable package.

Humidity

Humidity has been widely used in the electronics packaging industry as an acceleration mechanism. The operating environment of the usual packages vary from 30% up to 85%RH in tropical conditions. Hence, packages routinely use humidity as an acceleration mechanism. However, since the intended operating environment for the Glass-Silicon package is inside the living tissue, the corresponding humidity level is close to 100%. Hence humidity cannot be used as an acceleration mechanism.

Bias

Bias in combination with temperature and humidity (THB) has been used to accelerate the operating conditions of both CMOS and bipolar circuits. Inherently the bias generates currents and local heating which in turn reduces the actual humidity. As such, the bipolar circuits are always reverse biased during testing which is representative of the worst case scenario. At this point in time, we assume that the temperature rise due to operating electronics is sufficiently low not to cause any additional problems, and so we will not use bias in our initial tests.

Temperature

Almost all chemical processes which are characterized by an activation energy are temperature dependent. Moreover, diffusion into thin films also varies strongly with temperature. As such, one can use temperature as an acceleration mechanism, however the failure mechanism that is accelerated should be carefully determined. For instance, if the diffusion mechanism is accelerated one should be careful to make sure that the mechanism accelerated is the diffusion and not the dissolution of a material. Also as mentioned in the design of an accelerated test section the

material being tested should not decompose at the testing temperature unless the decomposition is proven to occur under the normal operating conditions.

Pressure

Pressure and temperature have been widely used (as in pressure cookers) to accelerate the effect of high temperature and high relative humidities. For instance, pressure vessels provide a more severe environment for testing than the usual accelerated conditions (85°C, 85%RH). There are several models derived to analyze this data and some state that with the use of pressure one can enhance acceleration [10]. For our specific tests, the dominant failure mode is the dissolution of silicon and pressure should not accelerate this failure mode. If we can stop the dissolution of silicon at higher temperatures (and this we believe we can accomplish) and create a condition where the dominant failure mode is caused by the diffusion of moisture into the package, then one can use pressure with temperature to accelerate the tests.

Concentration

Some accelerated tests for underwater devices include an increase in the concentration of the solution. Hence, to verify the activation energy for the dissolution of silicon we can use more concentrated solutions. The same effect could also be observed by having a silicon bonding region twice the size of the current one (600μm).

pH

Several implanted devices [11] have been analyzed by using different pH values. Under normal conditions, the body is a slightly basic environment with a pH close to 7.4, however in case of electrolysis the pH may vary. As such, almost all of the mentioned studies are performed to determine the effect of pH variations typically from 4 to 10. They are basically reliability studies where the effects of pH on corrosion has been investigated. These tests can be conducted only to observe the reliability of our packages in different pH environments.

A final note along the same lines is that the leak rates of hermetic packages can be used to determine their lifetimes for moisture penetration [12]. Compared to other acceleration models there are very few of these attempts and there also are a few that mention that the lifetime of the package had little to do with the gas-tightness of the package [13].

2.3.7 Time-To-Failure Modeling

For a material to fail under stress, a net amount of material must collect in or flow out of the region of failure. Using Fick's second law and doing the derivation [14] one can obtain the equation for the time to failure (TF):

$$TF = B\,(\xi)^{-n} \exp\left(\frac{Q}{kT}\right) \qquad \text{(Eq 1)}$$

where B is the process dependent parameter that depends only on the specifics of the flux divergence and the critical amount of material that must be accumulated or depleted before failure occurs. In general, n is termed as the stress dependence and the Q the activation energy.

2.3.8 Time-To-Failure Statistics

When identically processed materials are placed under stress, they will not fail exactly at the same time. The reason is that even for the same modeling equation there is a process dependent term (that appears as a constant) which will vary from sample to sample. This means that the time to failure is of interest as well as the distribution of the times to failure. Once the distribution of the times-to-failure is established, a probability density function can be constructed which will permit one to estimate the probability of estimating future failures. Historically, three probability density functions have been widely used to describe VLSI failures: exponential, Weibull, and lognormal. Since exponential is a special case of the Weibull, only the latter two will be mentioned in this section.

Lognormal distribution: The lognormal probability density function is defined as:

$$f(t) = \frac{1}{\sigma t\sqrt{2\pi}} \exp\{-[\frac{\ln(t) - \ln(t50)}{\sigma\sqrt{2}}]^2\} \qquad \text{(Eq 2)}$$

where t50 is the median time-to-failure and σ is the logarithmic standard deviation. The value σ is usually approximated by $\sigma = \ln\left(\frac{t50}{t16}\right)$ where t16 represents the time-to-failure for 16% of the units. Both t50 and t16 can be read directly from a cumulative failure probability F(t) plot on lognormal probability paper.

Weibull distribution: The Weibull probability density function is defined by :

$$f(t) = \left(\frac{\beta}{\alpha}\right)\left(\frac{t}{\alpha}\right)^{\beta-1} * \exp\left[-\left(\frac{t}{\alpha}\right)^{\beta}\right] \qquad \text{(Eq 3)}$$

where α is the characteristic time-to-failure and β is referred to as the shape (or dispersion) parameter. The values of α and β can be determined from a cumulative failure probability plot on Weibull probability paper.

2.3.9 Acceleration Factor

The concept and use of an acceleration factor are fundamental to the theory of accelerated testing. The acceleration factor, AF is defined as the ratio of the expected time-to-failure under normal operating conditions to the time-to-failure under accelerated stress conditions:

$$AF = \frac{(TF)_{op}}{(TF)_{stress}} \qquad \text{(Eq 4)}$$

Using Equation 1, one obtains :

$$AF = \left(\frac{\xi_{op}}{\xi_{stress}}\right)^{-n} \exp\left[\frac{Q}{K_B}\left(\frac{1}{T_{op}} - \frac{1}{T_{stress}}\right)\right] \qquad \text{(Eq 5)}$$

where the values of n and Q are determined under accelerated stress conditions. This equation allows one to model the acceleration factor without having to perform the years of testing implied by Eq 4. To go from the failure rate data taken under accelerated conditions to the predicted failure

rate under normal operating conditions, the following transformations are used for the lognormal and Weibull distributions:

$$(t50)_{operating} = AF\ (t50)_{stress}$$
$$(\sigma)_{operating} = (\sigma)_{stress} \qquad \text{(Eq 6)}$$

and

$$(\alpha)_{operating} = AF\ (\alpha)_{stress}$$
$$(\beta)_{operating} = (\beta)_{stress} \qquad \text{(Eq 7)}$$

Even though the characteristic time-to-failure for each distribution has been transformed by using the acceleration factor, it has been assumed that the dispersion parameter for each distribution does not change with stress. This serves as the definition for uniform stressing; that is, uniform stress accelerates the time-to-failure but does not change the dispersion of the time-to-failure data.

2.3.10 Conclusion

In this section we report on a literature study of accelerated tests that could be used for implantable devices. The fundamental definitions and precautions of an accelerated test are detailed. More specific focus is denoted to physics of failure approach in modeling the accelerated tests for an anodically bonded Glass silicon package. The predominant failure of the in-vitro tests mode is mentioned and the various ways to accelerate this mode is discussed from the available mechanisms that are published in literature. The most general models used in similar accelerated tests are also mentioned. In future reports we will more specifically discuss our approach to further testing of the hermeticity of the Glass-Silicon package.

2.4 The Design and Fabrication of a Relative Humidity Sensor

We have been using a dew point sensor to determine whether moisture has penetrated inside our packages in our accelerated tests. The main limitation of this device is that it can only detect whether water has condensed inside the package and that it does not exactly monitor the amount of humidity inside the package. We have proposed a system with which one can constantly monitor humidity from an implanted device with telemetry using a humidity sensor. With this in mind, we have investigated the possibility of a commercial humidity sensor. Most of the commercial humidity sensors operate up to a temperature of 120°C and are not reliable once exposed to high temperatures such as the anodic bonding temperature (320°C) used during the fabrication of the glass-silicon packages, also the commercial sensors are too large to fit inside our package. Another idea that was pursued was the use of a thin layer of polyimide on top of the dew point sensor which would convert it into a humidity sensor. After doing the calculations we found out that the dew point sensor has a very high parasitic capacitance to the substrate (12pF) as opposed to the one between the fingers (.2pF). For dew point measurements this is acceptable since the change after condensation is very drastic but it is not acceptable for humidity measurements. Hence, we have studied various methods and materials that are used in fabricating humidity sensors and decided on the IC compatible polyimide humidity sensor. The sensor is a parallel plate capacitive type humidity sensor in which polyimide layer after absorbing humidity will change its dielectric constant and hence the capacitance. In order to ease testing, we surveyed different types of polyimides and found out a type of polyimide that can be used to get a large change in capacitance for the entire range of humidity variations. This polyimide is typically used with a thickness of 300Å for display applications. In order to improve reliability and yield (i.e., to

prevent the pads from shorting each other) we have chosen to use 1000Å-thick films in our design. The device structure is shown in Figure 17 below.

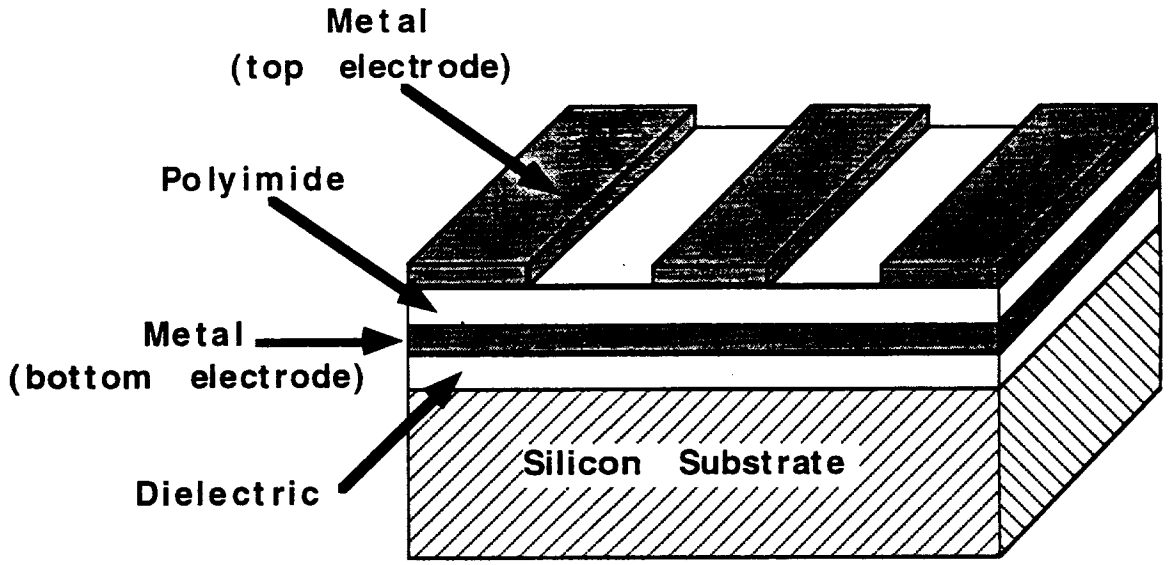

Figure 17: The cross sectional view of a polyimide parallel plate type capacitive sensor.

The design details of the relative humidity sensor are summarized in Table 8. Before integrating the humidity sensor into our packaging layout we wanted to characterize and calibrate the sensor. Hence, we have designed a layout consisting of 3 masks and fabricated the masks in house. We have recently started fabrication of the humidity sensor, but have not finished yet. We hope to finish fabrication of the sensor and characterize it in the coming quarter. With the use of the new autoclave we will perform aging studies on the relative humidity sensors before integrating them into our package design.

Table 8: The details of the humidity sensor.

Capacitor Plate Area	1 mm^2
Effective Area	0.5 mm^2
Polyimide Thickness	0.1 μm
Capacitance @0%RH (C_{dry})	146 pF
Capacitance @100%RH (C_{wet})	173 pF
Dynamic Range	0 to 100 % RH
Sensitivity (C_{dry} - C_{wet})/ C_{dry}	25 %

2.5 Telemetry Monitoring of Dew Point Inside the Package

One limitation of our current testing procedure, which consists of probing the dew point sensors from external pads, is the fact that this electrical testing is impossible once the probing pads are dissolved or covered with salt deposits. We then have to rely on visual observation to determine when failure occurs. Another limitation is the fact that for testing each device has to be handled separately, which is both time consuming and also increases the chances of mishandling which can lead to accidental failure. In order to overcome these limitations, we have been working on a telemetry measurement technique of dew point inside the package. This technique has not been implemented yet and some more work needs to be done before it will, but this section gives a presentation of the principles on which this telemetry monitoring is based.

2.5.1 Principles of the Measurement

The telemetry system is based on the electromagnetic coupling between a copper integrated coil placed inside the package under test, and an outside coil wired around the test tube in which the package will be soaking. When dew point forms on the integrated coil inside the package, the properties of this coil are changed. As we measure the impedance of the external coil, which is electromagnetically coupled to the first one, those property changes are detected. We should then be able to detect when dew point is formed inside the package.

The measurement setup is thus composed of 2 systems, seen on Figure 18:

1. The internal system, which is the integrated coil inside the package, which will be directly affected by water condensation or humidity increase inside the package.

2. The external system, which is a basic inductance in parallel with a capacitance resonant system, electromagnetically coupled to the internal system, and thus indirectly influenced by the changes inside the packages.

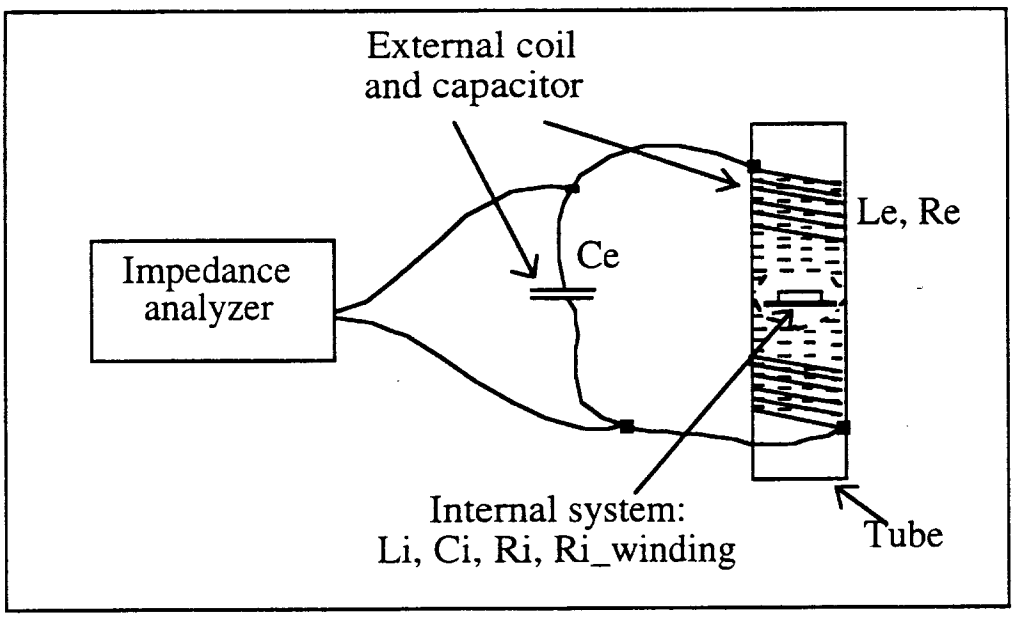

Figure 18: The experimental setup.

2.5.2 Theoretical Modeling and Derivations

The integrated copper coil as well as the external wire coil are modeled by an impedance in series with a resistance, those two in parallel with a capacitance. This capacitance is mostly due to the winding to substrate parasitic capacitance for the integrated coil (when it is dry), and to either a capacitance added in parallel or a parasitic wiring to wiring capacitance in the case of the external wired coil. Formation of dew-point inside the package, which deposits on the integrated coil, can be as a first approximation modeled by a resistance of low value (a few 10's of ohms) shorting the inductance. Figure 19 shows the complete modeling of the system.

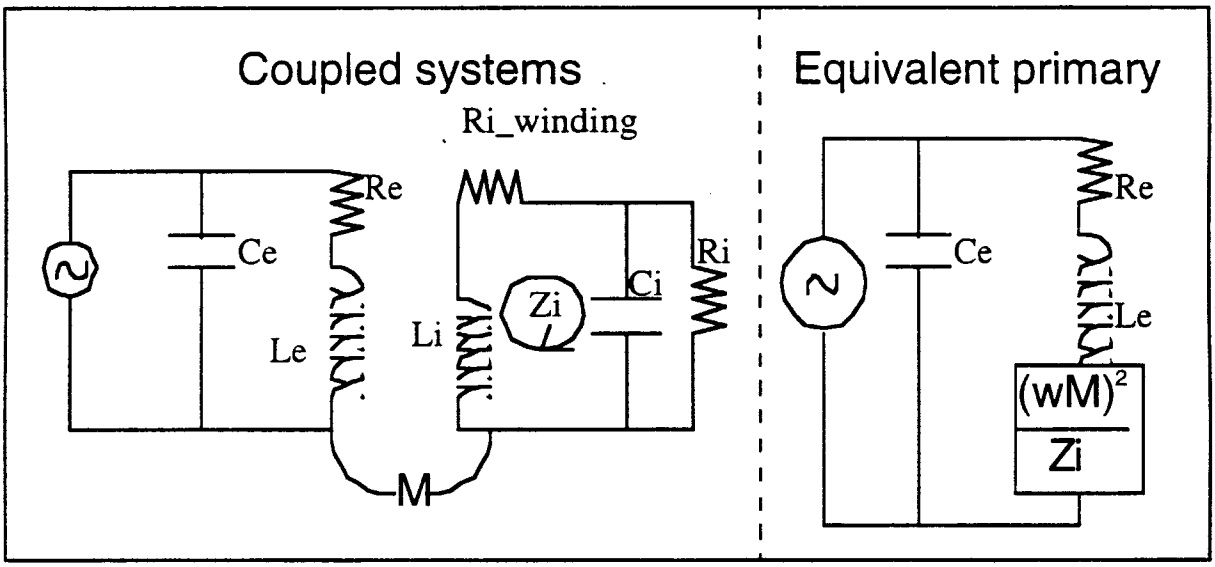

Figure 19: Electrical modeling of the system.

In order to optimize the design of both the integrated and the external coil, so that we have a maximum coupling and sensitivity to the changes inside the package due to dew-point formation, we derived the equations governing the system.

In all the following equations, we use the following parameters (all lengths in the equations have to be in meters):

For the integrated coil:

Ni	number of turns
wi	width of a turn
si	spacing between 2 turns
hi	electroplated thickness
Ai	average area of a turn
Lmax (Wmax)	maximum length (width)
Lmin (Wmin)	minimum length (width)
Ci	winding/substrate capac.
Li	inductance
Ri_winding	winding resistance
fo_int	resonance frequency
wo_int	resonance pulsation
tox	dielectric coil/subst. thick.
Ri	modeling of the humidity

For the external coil (single layer solenoid):

Ne	number of turns
ne	number of turns per meter
de	diameter of one turn
le	length of the solenoid
Le	inductance
Re	winding resistance
Ae	cross sectional area
Ce	capacitance
fo_ext	resonance frequency
wo_ext	resonance pulsation
α,β	angles determining position inside the solenoid

For the coupling and other parameters:

Bie magnetic field created in the internal coil area by a current in the external coil
μo free space permeability (=4πe-7 H/m)
M mutual inductance between the 2 coils
ϵ_ox oxide permittivity (=3.7*8,85e-12 F/m)
ρ_Cu copper resistivity (=2.0e-8 Ω*m)
μ_core here there is no core so μ_core=1

We have the following equations for the coupling of the 2 systems, when the internal coil is placed in the middle of the external coil, the winding planes being parallel for a better coupling:

$$Zi = j\omega L_i + R_{i\_winding} + \frac{1}{j\omega C_i + \frac{1}{R_i}}$$

$$Ze = \frac{1}{j\omega C_e + \frac{1}{j\omega L_e + R_e + \frac{(\omega M)^2}{Zi}}}$$

The mutual inductance is given by:

$$M = \frac{N_i A_i B_{ie}}{i_e} \quad with \quad B_{ie} = \frac{\mu_o N_i}{2l_e}(\cos\alpha - \cos\beta)$$

We get:

$$M = \frac{N_i A_i N_e \mu_o}{\sqrt{d_e^2 + l_e^2}} \quad with \quad A_i = \frac{L_{max} W_{max} + L_{min} W_{min}}{2}$$

The coupling coefficient is given by $k = \frac{M}{\sqrt{L_i L_e}}$

The parameters concerning the external solenoid are given by:

$$L_i = \frac{\mu_o N_e^2 A_e}{l_e + 0.45 d_e} \quad Henry$$

If the capacitance of the external circuit is tuned so that the resonance frequencies of the external and the internal circuits are the same, we have Ce given to satisfy

$$\omega_{o\_int} = \frac{1}{\sqrt{L_i C_i}} \quad = \quad \omega_{o\_ext} = \frac{1}{\sqrt{L_e C_e}}$$

The parameters concerning the internal integrated coil are given by:

$$L_i = 9.21e-7 \cdot N_i^2 \cdot \mu_{core}\left[(L_{coil}+W_{coil})\cdot \log_{10}\left(\frac{8L_{coil}W_{coil}}{N_i w_i + N_i h_i}\right) - k1 - k2\right]$$

where

$$L_{coil} = \frac{l_{i\_min} + l_{i\_max}}{2} \quad , \quad W_{coil} = \frac{w_{i\_min} + w_{i\_max}}{2}$$

$$k1 = L_{coil}\cdot \log_{10}\left(L_{coil} + \sqrt{L_{coil}^2 + W_{coil}^2}\right) \quad , \quad k2 = W_{coil}\cdot \log_{10}\left(W_{coil} + \sqrt{L_{coil}^2 + W_{coil}^2}\right)$$

We can also derive the winding resistance and the winding to substrate capacitance (for now we will consider the winding to winding capacitance negligible):

$$Winding\_length = 2\cdot \sum_{k=0}^{Ni-1}(w_{i\_max} + l_{i\_max} - 4k(s_i + w_i))$$

$$R_{i\_winding} = \frac{\rho_{Cu}\cdot Winding\_length}{w_i \cdot h_i} \quad , \quad C_i = \frac{\in_{ox}\cdot Winding\_length \cdot w_i}{t_{ox}}$$

2.5.3 Current Work

Using the equations given in the previous section, we simulated the impedance measurement we expect from the external coil. These simulations should enable us to optimize the design of the integrated coil and of the external coil. It should be noted that for simplicity the previous calculations were made considering air inside the external coil. As we will test the packages inside water, we have to take this into account. The presence of water inside the external coil strongly modifies its behavior and reduces sensitivity to the coupling with the integrated coil. We are now working on making some measurements and experimentation to make the technique suitable to aqueous environment.

3. PLANS FOR THE COMING QUARTER

In the coming quarter we will continue our activities in the various areas. One of the tasks that we would like to start as soon as possible is to implant a package with a humidity sensor so we can monitor the humidity inside the animal. This has not yet been done partly because we are in the process of fabricating the humidity sensors, and partly because we have not yet been able to hire a new student to work on this aspect of the project. This latter problem will be resolved at the beginning of the Fall term. We will also start working on our silicon-silicon package technology as we had presented in the proposal.

References

[1] E. J. Charlson, R. Sabeti, E. M. Charlson and H. K. Yasuda, "Protective coating of integrated circuits for operation in corrosive environments", *Mat. Res. Soc. Symp. Proc.* Vol.154, pp. 91-96, 1989.

[2] W. Nelson, *Accelerated Testing, Statistical Models, Test Plans, and Data Analyses*, John Wiley &Sons, New York 1990.

[3] K. D. Wise and R. H. Weisman, "Thin films of glass and their application to biomedical sensors", *Med. Biol. Eng.*, vol.9, pp. 339-350, July 1971.

[4] ASTM F1634-95, "Standard Practice for In-Vitro Environmental Conditioning of Polymer Matrix Composite Materials and Implant Devices".

[5] B. B. Owens, *Batteries for Implantable Biomedical Devices*, Plenum Press, New York 1986.

[6] W. Q. Meeker, and M. J. LuValle, "An accelerated life test model based on reliability kinetics", *Technometrics*, vol. 37, no.2, pp. 133-46, May 1995.

[7] P. E. K. Donaldson and B. J. Aylett, "Aspects of silicone rubber as encapsulant for neurological prostheses Part 3: adhesion to mixed oxides", *Med. & Biol. Eng.& Comput.*, vol. 33, pp. 725-27, 1995.

[8] P. E. K. Donaldson and B. J. Aylett, "Aspects of silicone rubber as encapsulant for neurological prostheses Part 2: adhesion to binary oxides", *Med. & Biol. Eng.& Comput.*, vol. 33, pp. 285-92, 1995.

[9] P. E. K. Donaldson, "Aspects of silicone rubber as encapsulant for neurological prostheses Part 4: Two part rubbers", *Med. & Biol. Eng.& Comput.*, vol. 35, pp. 283-6, 1997.

[10] D. S. Peck, "Comprehensive model for humidity testing colleration", *Int'l. Rel. Phys. Symp.*, pp. 44-50, 1986.

[11] K. Kreider, "Iridium oxide thin film stability in high temperature corrosive solutions", *Sensors and Actuators B*, vol.5, pp. 165-69, 1991.

[12] A. DerMarderosian and V. Gionet, "Water vapor penetration rate into enclosures with known air leak rates", pp. 179-186.

[13] P. E. K. Donaldson and E. Sayer, "Osmotic pumping of non-hermetic neuroprosthetic implants", *Med. & Biol. Eng.& Comput.*, vol. 19, pp. 483-5, 1981.

[14] M.G. Pecht, L. T. Nguyen and E. B. Hakim, "*Plastic Encapsulated Microelectronics Materials, Processes, Quality, Reliability and Applications*", John Wiley & Sons, New York, 1995.

some important references not mentioned in this section:

[15] P. E. K. Donaldson, "The encapsulation of microelectronic devices for long term surgical implantation", *IEEE Trans. Biomed Eng.*, vol.23, no.4, pp. 281-5, 1976.

[16] L. Bowman and J. D. Meindl, "The packaging of implantable integerated sensors", *IEEE Trans. Biomed Eng.*, vol.33, no.2, pp. 248-55, 1986.

[17] P. E. K. Donaldson and E. Sayer, "A technology for implantable hermetic packages. Part 1: Design and materials", *Med. & Biol. Eng.& Comput.*, vol. 19, pp. 398-402, 1981.

[18] P. E. K. Donaldson and E. Sayer, ", "A technology for implantable hermetic packages. Part 2: An implementation", *Med. & Biol. Eng.& Comput.*, vol. 19, pp. 403-5, 1981.

[19] W. W. Weick, "Acceleration factors for IC leakage current in a steam environment", *IEEE Trans. Rel.*, vol. R-29, no. 2, pp. 109-15, 1980.

[20] N. Sinnadurai, "Plastic packaging is highly reliable", *IEEE Trans. Rel.*, vol. 45, no. 2, pp. 184-93, 1996.

[21] M. F. Nichols, "The challenges for hermetic encapsulation of implanted devices - A review", *Crit. Revs. Biomed. Eng.*, vol. 22, no. 1, pp. 39-67, 1994.

[22] M. L. White, "Encapsulation of integrated circuits", *Proc. IEEE* , vol. 57, pp. 1610-15, 1969.

[23] J. W. Lathrop, D. C. Hawkins, J. L. Prince, and H. A. Walker, "Accelerated stress testing of terrestrial solar cells", *IEEE Trans. Rel.*, vol. R-31, no. 3, pp. 258-65, 1982.

[24] N. E. Lycoudes, "The reliability of plastic microcircuits in moist environments", *Solid State Tech.*, p. 53-68, 1978.

[25] W. J. Mcgarvey, "Autoclave vs. 85°C/85% R. H. testing - A comparison", *Int'l Rel Phys Symp*, pp. 136-42, 1979.

[26] D. F. Lovely, M. B. Olive and R. N. Scott, "Epoxy moulding system for the encapsulation of microelectronic devices for implantation", *Med. & Biol. Eng.& Comput.*, vol. 24, pp. 206-8, 1986.